
Prompt-Aware Adapter: Towards Learning Adaptive Visual Tokens for Multimodal Large Language Models

Yue Zhang Hehe Fan Yi Yang
School of Computer Science and Technology
Zhejiang University

Abstract

To bridge the gap between vision and language modalities, Multimodal Large Language Models (MLLMs) usually learn an adapter that converts visual inputs to understandable tokens for Large Language Models (LLMs). However, most adapters generate consistent visual tokens, regardless of the specific objects of interest mentioned in the prompt. Since these adapters distribute equal attention to every detail in the image and focus on the entire scene, they may increase the cognitive load for LLMs, particularly when processing complex scenes. To alleviate this problem, we propose prompt-aware adapters. These adapters are designed with the capability to dynamically embed visual inputs based on the specific focus of the prompt. Specifically, prompt-aware adapters utilize both global and local textual features to capture the most relevant visual clues from the prompt at both coarse and fine granularity levels. This approach significantly enhances the ability of LLMs to understand and interpret visual content. Experiments on various visual question answering tasks, such as counting and position reasoning, demonstrate the effectiveness of prompt-aware adapters.

1 Introduction

Recent advances in Large Language Models (LLMs) [1, 2, 3, 4, 5] have significantly enhanced their performance across various natural language processing tasks. These models are able to perform language comprehension and logical reasoning, enabling them to handle complex linguistic functions such as summarizing texts, answering questions, processing dialogues, and composing new essays or articles. However, LLMs are inherently limited by their inability to process visual information. This has led to the development of Multimodal Large Language Models (MLLMs) [6, 7, 8, 9, 10], which expand upon LLMs by incorporating visual processing abilities. MLLMs offer a more holistic understanding and interaction by synthesizing both textual and visual data, thereby broadening their utility in diverse real-world applications.

To equip LLMs with visual perception ability, MLLMs typically employ a trainable adapter that connects a frozen visual encoder and a frozen LLM. Adapters play a crucial role in bridging the gap between vision and language, enabling profound visual understanding while leveraging the powerful reasoning capabilities of LLMs. However, most existing adapters [11, 12, 13, 14, 15, 10, 16, 17] approach visual patches as if they were words, and directly translate these patches into tokens comprehensible to LLMs (e.g., through linear projection), regardless of the specific objects of interest in the prompt. These prompt-unaware adapters may enable LLMs to correctly analyze simple images but could struggle to understand complex scenes. As shown in Fig. 1, no matter the query is “is there a pool in this image” or “how many drinks are on the table”, these adapters consistently convert the image into the same tokens. Consequently, the subsequent LLMs have to independently parse the scene to deduce the spatial context and shift attention to “pool” or “drinks” entirely on their own.

A few studies have explored using prompts to guide the behavior of adapters. For instance, Vision-LLM [18] and Flamingo [19] employs the cross-attention mechanism to learn adaptive visual tokens,

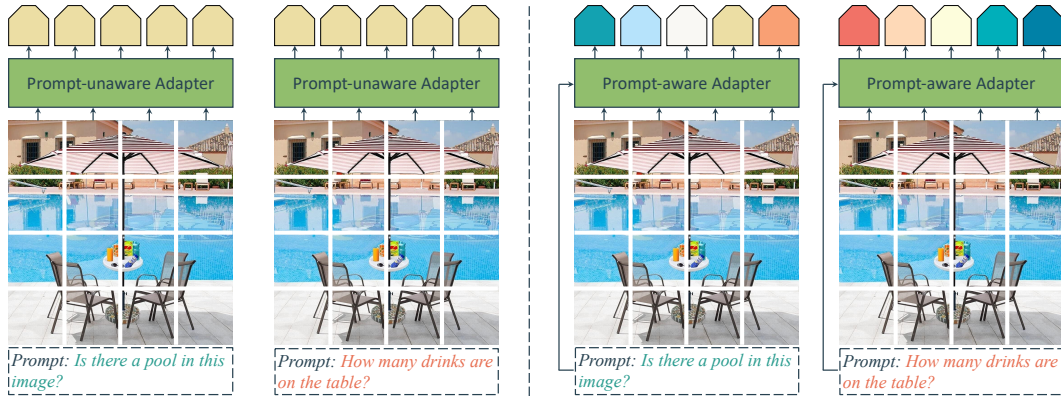


Figure 1: Illustration comparing prompt-unaware and prompt-aware adapters. **Left:** Prompt-unaware adapter treats visual patches as a kind of words and directly converts these patches into “readable” tokens for LLMs, without considering the specific objects of interest. In this case, whether the question involves “pool” or “drinks,” they consistently generate the same tokens and allocate equal attention to every detail in the scene, which may increase the cognitive load for LLMs. **Right:** Prompt-aware adapter leverages prompts to collect the most relevant visual clues and generate adaptive tokens, thus enhancing the ability of LLMs to understand and interpret visual content.

where prompt words serve as the query and image patches are treated as the key and value. Instruct-BLIP [20] first injects the prompt information into learned queries [21] (via self-attention) and then uses cross-attention to gather visual clues. These cross-attention-based adapters encounter two main challenges. First, they search for visual clues at the word level, thereby neglecting global information for capturing an overview of the prompt-related region. Second, the use of the softmax function in cross-attention normalizes attention distribution from word to patch such that the total attention allocated to each word equals 1. This implies that every word in the prompt, including function words like “a”, “the” and “is”, is forced to correspond to a specific region in the image. Because these irrelevant words may correspond to different regions each time, this unrealistic assumption may lead adapters to produce unstable visual tokens, inevitably causing significant confusion for LLMs.

In this paper, we produce a prompt-aware adapter to adaptively embed visual inputs based on the prompt’s global and local representations. Our adapter comprises two key components: prompt-aware global attention and prompt-aware local attention. The global attention is designed to capture coarse-grained, prompt-related visual perceptions, while the local attention focuses on refining responses to specific, fine-grained regions of interest. This dual approach allows adapters to effectively uncover visual contexts and shift attention to relevant areas as needed. We conducted extensive experiments on the COCO-QA [22] and MME [23] datasets. Compared to the prompt-unaware baseline, our method shows significant improvements on COCO-QA, enhancing object classification, counting, color recognition, and positional reasoning by 7.71%, 18.42%, 12.84%, and 9.51%, respectively. On the MME dataset, it boosts the total scores for perception tasks and cognition tasks by 59.43% and 46.91%, respectively. Our method demonstrates superior performance in handling complex scenarios and parsing intricate problems, effectively sensing prompts and capturing informative details necessary for answering questions. The contributions are as follows:

- Among the early efforts, we conduct a comprehensive study on the impact of prompts on adapters. Our research reveals that prompt-independent adapters may be not sufficient to capture the most informative visual clues for visual understanding. Furthermore, existing prompt-relevant adapters still suffer from issues such as failing to focus on crucial words in prompts or adequately aligning visual and semantic elements.
- We propose prompt-aware adapters that dynamically embed visual inputs based on prompts at both coarse and fine granularities. Our method provides effective and convenient attention mechanisms for existing adapter-empowered MLLMs.
- Experiments on complex scene understanding applications demonstrate that the proposed method effectively improves the visual perception and reasoning capabilities of MLLMs.

2 Related Work

Multimodal Large Language Models and Adapters. The integration of the perceptual abilities of vision models [24, 25, 26, 27] with the reasoning capabilities of LLMs [1, 28, 29, 30, 31, 3] has given rise to Multimodal Large Language Models (MLLMs) [32, 33, 34, 35, 36, 37]. In MLLMs, visual signals are converted into tokens that LLMs can understand, typically using adapters. For example, MLLMs such as LLaVA [11], Shikra [13], MiniGPT [12], Matters [14], PandaGPT [15], Kosmos [10], and InfMLLM [16] utilize linear projection adapters. QWEN-VL [38] and mPIUG-Owl [39] employ Perceiver-like architectures [40] as adapters. Since the introduction of the Q-Former in BLIP-2 [21], many MLLMs [41, 42] have adopted it as an adapter for modal alignment. The visual descriptions generated by the aforementioned prompt-independent adapters typically encompass the entire image, without emphasizing the specific visual details relevant to the prompt. VisionLLM [18], Flamingo [19], and subsequent studies [43, 44] utilize cross-attention adapters to improve prompt-aware capabilities. InstructBLIP [20] and Cheator [45] incorporate prompt information into learned queries using self-attention and then employ cross-attention to collect visual clues. These adapters often struggle with issues such as failing to focus on crucial words in prompts or adequately aligning visual and semantic elements. In this paper, we introduce a new type of adapter designed to align visual signals with textual semantics for MLLMs.

Attention Mechanisms. The attention mechanism [46] enables vision-language models to focus on relevant information within the input while minimizing focus on irrelevant details. Its effectiveness and interpretability have inspired numerous subsequent studies [47, 48, 49]. For example, [50] introduces both hard and soft attention mechanisms that automatically learn to describe the contents of images. Additionally, in the Visual Question Answering (VQA) task, it is crucial to focus on the relevant parts of both the image and the question. Consequently, Co-Attention [51] was developed to facilitate simultaneous attention learning across multiple inputs (i.e., image and text). Self-Attention [52] enables interactions between different positions within a single input sequence, thereby capturing content that is relatively more important. Drawing from sources such as [52, 53, 54], the Transformer [55], recognized as a foundational component of large models, incorporates Scaled Dot-Product Attention and Multi-Head Attention. Cross-Attention [56] has been developed within the Transformer [55] architecture to facilitate interaction between two different sequences. To enhance the interaction between images and text, we propose global and local attention mechanisms that automatically focus on the visual content of interest mentioned in the text.

3 Proposed Method

In this section, We first provide a brief overview of existing adapters for the visual perception of Multimodal Large Language Models (MLLMs). Then, we describe how the proposed prompt-aware adapter enables MLLMs to effectively uncover visual context and adaptively shift attention for enhancing visual reasoning.

3.1 Preliminary: MLLM and Adapter

MLLM is an advanced type of artificial intelligence model that processes and understands information from multiple types of data, such as text, images, and sometimes audio or video. This allows the model to perform tasks that involve more than one mode of communication, providing a richer understanding of the content than the text-only LLM. MLLMs integrate capabilities from different domains. For example, they can extract meaning from both the text in an image caption and the visual content of the image itself. This is particularly useful in applications such as image captioning, Visual Question Answering (VQA) and video understanding.

In MLLMs, a specialized module called adapter is commonly employed to enhance the model’s capability to process and integrate information from different modalities. Adapters are particularly valuable because they allow pre-trained models to be adapted to new tasks or modalities without the need for extensive retraining of the entire model. Formally, for a given visual input, a frozen visual encoder (such as ViT and Q-Former) is typically employed to extract the visual features $\mathbf{X} \in \mathbb{R}^{N \times C}$, where N represents the number of patches and C denotes the number of feature channels. Because these visual features are not directly comprehensible to the subsequent LLM, the adapter is trained to

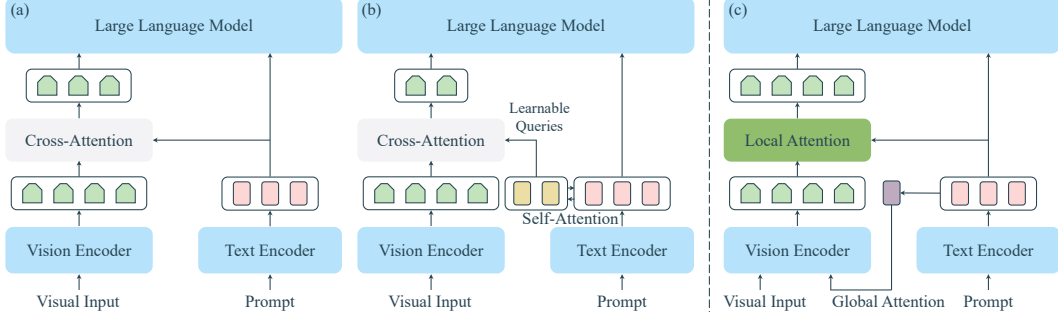


Figure 2: Illustration comparing the cross-attention (left) and proposed (right) adapters. (a) Methods like VisionLLM [18] and Flamingo [19] utilize text features as queries and visual features as keys and values in cross-attention. It assumes that each word in the prompt corresponds to specific regions. The number of converted visual tokens is equal to that of text features. (b) InstructBLIP [20] first injects prompt information into learnable queries via self-attention, and then employs cross-attention. It assumes that each query in the learnable queries corresponds to specific regions. The number of converted visual tokens is equal to that of learnable queries. (c) Our adapter comprises global and local attention components. Due to the new attention calculation mechanism used in local attention, the number of converted visual tokens remains unchanged.

translate them into tokens that the LLM can understand as follows,

$$\mathbf{X}' = \text{Adapter}(\mathbf{X}; \theta), \quad (1)$$

where θ is the learnable parameters of the adapter, $\mathbf{X}' \in \mathbb{R}^{N' \times C'}$ and N' represents the number of converted tokens and C' denotes the dimension of the LLM's input. In most MLLMs, the adapter is implemented as a linear projection layer that projects visual features into the textual feature space [11, 12, 14, 15, 13]. Additionally, the adapter in Honeybee [17] first applies a convolution to convert visual features and then downsamples them, resulting in $N' < N$. However, no matter linear projection or convolution, these adapters distribute equal attention to every detail in the visual input and focus on the entire scene, regardless of the specific objects of interest mentioned in the prompt, converting visual input to invariant tokens. In this case, these prompt-unaware adapters may struggle to effectively convert complex scenes for its subsequent LLM.

3.2 Prompt-Aware Adapter

To translate informative visual tokens for LLMs, we can use prompts to guide the behavior of adapters. Suppose $\mathbf{Y} \in \mathbb{R}^{M \times D}$ is the prompt, where M represents the number of words in the prompt and D denotes the dimension of the word embedding. This mechanism can be formulated as follows,

$$\mathbf{X}' = \text{Adapter}(\mathbf{X}, \mathbf{Y}; \theta). \quad (2)$$

There are many ways to implement Eq. (2). As shown in Fig 2, VisionLLM [18] and Flamingo [19] utilize text features as queries and visual features as keys and values in cross-attention processes to facilitate modal interaction. InstructBLIP [20] first incorporates prompt information into learned queries through self-attention, and then employs cross-attention to collect visual clues. In summary, these methods are based on cross-attention, which can be formulated as follows,

$$\mathbf{X}' = \text{softmax}\left(\frac{\mathbf{Q} \cdot \mathbf{K}^T}{\sqrt{E}}\right) \cdot \mathbf{V}, \quad \mathbf{Q} = \mathbf{Y} \cdot \mathbf{W}_q, \quad \mathbf{K} = \mathbf{X} \cdot \mathbf{W}_k, \quad \mathbf{V} = \mathbf{X} \cdot \mathbf{W}_v, \quad (3)$$

where $\mathbf{W}_q \in \mathbb{R}^{D \times E}$, $\mathbf{W}_k \in \mathbb{R}^{C \times E}$, $\mathbf{W}_v \in \mathbb{R}^{C \times E}$ and \cdot denotes matrix multiplication. In this paper, we use the lowercase softmax to indicate that the function is applied at each row. This mechanism results in two outcomes:

- **Attention.** Because the use of the softmax function in cross-attention normalizes the attention distribution from each word to all patches, the total attention allocated to each word equals 1. Specifically, if \mathbf{a}_{ij} represents the attention of the i -th word to the j -th patch, then $\sum_{j=1}^N \mathbf{a}_{ij} = 1$.

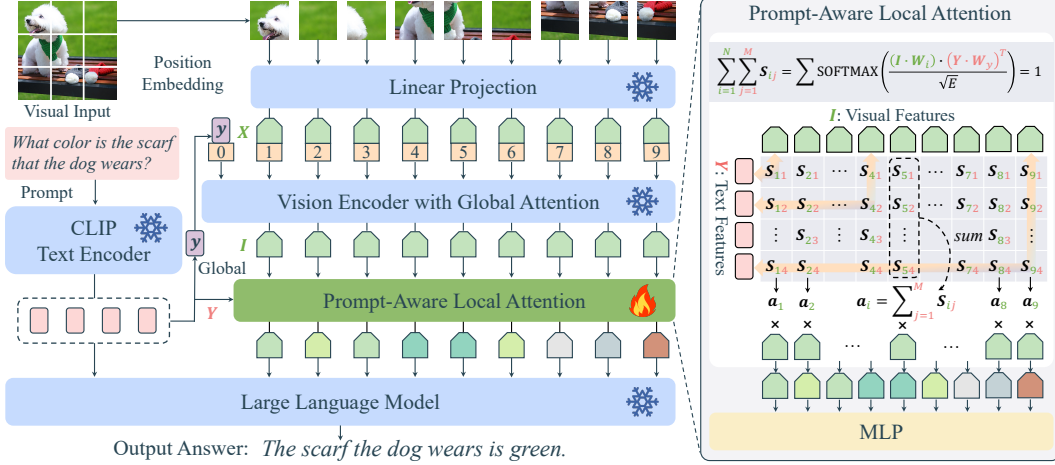


Figure 3: Illustration of the proposed prompt-aware adapter. The adapter consists of a global attention component and a local attention component. The global attention, integrated into the visual encoder, is designed to capture coarse-grained, prompt-related visual perceptions. Meanwhile, the local attention focuses on refining responses to specific, fine-grained regions of interest.

- **Output.** Because the prompt \mathbf{Y} serves as the query in cross-attention, it leads to $\mathbf{X}' \in \mathbb{R}^{M \times E}$. This indicates that the number of converted visual tokens is M (the number of words in the prompt), rather than N (the number of patches in the visual input).

This suggests that every word in the prompt, including function words like “a”, “an”, “the”, “is” and “are”, is forced to correspond to a specific region in the image. Given that these irrelevant words might correspond to different regions each time, this unrealistic assumption can cause adapters to generate unstable visual tokens, leading to significant confusion for LLMs.

Global Attention. To extract the most informative clues, we propose the prompt-aware adapter (shown in Fig. 3). The adapter consists of a prompt-aware global attention component and a prompt-aware local attention component. The global attention component searches for visual clues at the scene level, aiming to capture an overview of the region related to the prompt. To this end, we first utilize CLIP’s text encoder to extract the global feature of the prompt. Second, we employ a learned projection layer to map the global feature into the same space as the visual patch, i.e., $\mathbf{y} \in \mathbb{R}^{1 \times C}$. Third, the global feature of the prompt is appended to the visual patches, resulting in $[\mathbf{X}; \mathbf{y}] \in \mathbb{R}^{(N+1) \times C}$. Fourth, self-attention is employed to allow the adapter to incorporate the global prompt information, which is as follows,

$$\mathbf{I} = \text{SelfAttention}([\mathbf{y}; \mathbf{X}]). \quad (4)$$

In this way, a coarse extraction of visual clues mentioned in the prompt is conducted. Finally, the global attention discards the prompt representation at the last position, yielding N visual features, i.e., $\mathbf{I} \in \mathbb{R}^{N \times C_i}$, where C_i is the feature dimension.

Local Attention. Global attention reflects the overall correlation between the visual input and prompt. To capture local details, we design a local attention component. First, local attention calculates a similarity matrix $\mathbf{S} \in \mathbb{R}^{N \times M}$ between text and visual features, as follows,

$$\mathbf{S} = \text{SOFTMAX}\left(\frac{(\mathbf{I} \cdot \mathbf{W}_i) \cdot (\mathbf{Y} \cdot \mathbf{W}_y)^T}{\sqrt{E}}\right) \quad (5)$$

where $\mathbf{W}_i \in \mathbb{R}^{C_i \times E}$ and $\mathbf{W}_y \in \mathbb{R}^{D \times E}$. Here, we use the capital SOFTMAX to denote that the function is applied to the entire matrix. Compared to the softmax function used in Eq. (3), SOFTMAX suggests that each word may or may not correspond to a visual patch in the scene, and similarly, each patch may or may not correspond to a word in the prompt. This assumption is more flexible and realistic than that of cross-attention.

Second, the sum of each row ($\mathbb{R}^{1 \times M}$) in \mathbf{S} can be interpreted as the correlation between a specific patch and the entire prompt description. Therefore, we calculate the weight of each visual patch by

summing all attention focused on it, as follows,

$$\mathbf{a}_i = \sum_{j=1}^M \mathbf{S}_{ij}, \quad \mathbf{X}' = \text{MLP}(\mathbf{a}^T \cdot \mathbf{I}), \quad (6)$$

where $\mathbf{a} \in \mathbb{R}^{1 \times N}$. Then, local attention is applied to visual features. This process produces prompt-aware visual tokens. Finally, a multilayer perceptron (MLP) is employed to transform them.

Our method intrinsically differs from the cross-attention mechanism described in Eq. (3). In cross-attention, prompt features \mathbf{Y} function as \mathbf{Q} (queries) and visual features \mathbf{X} as \mathbf{K} (keys) and \mathbf{V} (values). Here, each text token distributes its attention across visual patches such that the total sums to 1. This means that even function words (like conjunctions and prepositions) must have their similarity scores with all visual tokens collectively equal 1. This requirement is impractical, as it assumes that every text token is equally significant in directing attention to visual cues. The proposed local attention mechanism ensures that $\sum_{i=1}^N \sum_{j=1}^M \mathbf{S}_{i,j} = 1$. As a result, text tokens that are more relevant to the visual context (and have higher similarity scores) exert greater influence on visual encoding. This approach, akin to emphasizing certain words in a sentence when reading aloud, allows for the extraction of prompt-related visual features in a more detailed and nuanced manner. In summary, there are two differences between cross-attention and the proposed local attention.

- **Attention.** The cross-attention implies that each word corresponds to a specific region, whereas local attention does not enforce such a correspondence.
- **Output.** The cross-attention produces M (the number of words in the prompt) visual tokens, whereas local attention generates N (the number of patches in the visual input) tokens.

4 Experiments

4.1 Implementation Details

Network Details. In this paper, we utilize the open-sourced LLaMA2 (7B) model [57] as our Large Language Model (LLM). We employ the text encoder from CLIP [27] to ensure that the extracted text features closely align with the corresponding visual features in the embedding space. ViT-g/14 from EVA-CLIP [58] is used as the vision encoder. The global text token is injected into the vision encoder to conduct prompt-aware global attention. The use AdamW [59] as the optimizer, with $\beta_1 = 0.9$, $\beta_2 = 0.999$, and a weight decay rate of 0.05. The learning rate is linearly warmed up from 10^{-6} to 8×10^{-5} over the first 1,000 steps to accelerate model convergence. This is followed by a cosine decay of the learning rate to a minimum of 10^{-5} . The training is set to a maximum of 50 epochs, with 1,000 iterations per epoch. The model is trained with a batch size of 4, across a period of 3 days on a single NVIDIA RTX A6000 GPU.

Training Details and Datasets. Following [57, 12], the conversation template is as follows,

$[INST] \langle \text{Img} \rangle \langle \text{Image Feature} \rangle \langle /\text{Img} \rangle [\text{Task Identifier}] \langle \text{Prompt Feature} \rangle [/INST]$

where $[INST]$ and $[/INST]$ represent the user role and chat assistant, respectively. During training, the $\langle \text{Image Feature} \rangle$ is replaced with the visual embeddings, and the $\langle \text{Prompt Feature} \rangle$ is substituted with textual prompt embeddings. The $[\text{Task Identifier}]$ is replaced based on specific circumstances (e.g., $[vqa]$ and $[caption]$), making our model more adept at understanding multiple tasks.

We initialize our model with the pre-trained parameters of MiniGPT-V2 [12]. MiniGPT-V2 has demonstrated impressive performance across multiple tasks, having undergone three stages of training on various fine-grained datasets [60, 61, 62, 63, 64, 65, 66, 67, 68, 69, 70, 71, 72, 73]. We fine-tune the model on downstream tasks at a low cost to validate the effectiveness of our method. Our model is trained on the COCO-QA dataset [22], which includes a mix of question-answer pairs covering object classification, color recognition, counting, and positional reasoning. The training image-text pairs account for around 67%, and the remaining pairs are used for the zero-shot image-to-text generation task. Throughout the entire training process, the text encoder, global prompt-aware vision encoder, and LLM remain frozen. Only the local prompt-aware vision adapter and additional projection layers are fine-tuned. Evaluation is primarily conducted on the COCO-QA [22] test dataset and the MME [23] benchmark. The latter includes 10 perceptual (i.e., existence, count, position, color, poster, celebrity, scene, landmark, artwork, and OCR) and 4 cognitive (i.e., commonsense reasoning, numerical calculation, text translation, and code reasoning) tasks.



Figure 4: Visualization of prompt-aware global and local attention. Global attention spans the entire prompt content, while local attention concentrates predominantly on the specific object in question.

Table 1: Quantitative results of 10 perception tasks on the MME [23] benchmark. Evaluation metric is scores for correct answers, with higher scores indicating better performance. *: frozen, \checkmark : fine-tuned. The best and second-best scores are highlighted in bold and underlined, respectively.

Method	Existence	Count	Position	Color	Poster	Celebrity	Scene	Landmark	Artwork	OCR	Total
MiniGPT-4 [41]	68.33	55.00	43.33	75.00	41.84	54.41	71.75	54.00	60.50	57.50	581.66
PandaGPT [15]	70.00	50.00	50.00	50.00	76.53	57.06	118.00	69.75	51.25	50.00	642.59
ImageBind-LLM [74]	128.33	60.00	46.67	73.33	64.97	76.47	113.25	62.00	70.75	80.00	775.77
VPGTrans [75]	70.00	85.00	63.33	73.33	84.01	53.53	141.75	64.75	77.25	77.50	790.45
LaVIN [76]	185.00	88.33	63.33	75.00	79.59	47.35	136.75	93.50	87.25	107.50	963.60
mPLUG-Owl [39]	120.00	50.00	50.00	55.00	136.05	100.29	135.50	<u>159.25</u>	96.25	65.00	967.34
LRV-Instruction [77]	165.00	111.67	<u>86.67</u>	165.00	139.04	<u>112.65</u>	147.98	160.53	101.25	<u>110.00</u>	1299.79
BLIP-2 [21]	160.00	<u>135.00</u>	77.33	148.33	<u>141.84</u>	105.59	145.25	138.00	136.50	<u>110.00</u>	1293.84
Flamingo [19]	70.00	60.00	46.67	73.33	41.84	57.06	68.00	62.00	60.50	65.00	604.40
Multimodal-GPT [43]	61.67	55.00	58.33	68.33	57.82	73.82	68.00	69.75	59.50	82.50	654.72
InstructBLIP [20]	185.00	143.33	66.67	<u>153.33</u>	123.81	101.18	<u>153.00</u>	79.75	<u>134.25</u>	72.50	1212.82
Linear \checkmark	88.33	35.00	20.00	43.33	24.82	93.82	74.75	108.75	41.50	27.5	557.82
Q-Former* + Linear \checkmark	83.18	49.45	50.66	68.95	55.05	55.68	49.93	53.02	30.29	49.54	545.78
Q-Former \checkmark + Linear \checkmark	65.00	33.22	51.66	54.21	42.70	52.60	73.75	73.04	52.13	72.50	570.84
Cross-Attention \checkmark	91.66	63.33	39.99	21.66	57.14	38.23	110.25	99.25	76.75	70.00	668.29
Ours	185.00	<u>135.00</u>	99.99	99.99	144.89	141.47	159.00	145.15	132.00	132.50	1375.02

4.2 Evaluation

Attention Visualization. To demonstrate the effectiveness of the proposed method, we visualize global and local attention in Fig. 4. The global attention map effectively targets entire regions of the image that semantically align with the entire prompt sentence. The local attention map, associated with the question, highlights its ability to explore fine-grained semantics when extracting visual clues.

Quantitative Results. For quantitative evaluation, we exclusively consider questions with precise and concise answers, due to the statistical challenges posed by open-ended responses from MLLMs [23, 3, 11]. First, we compare our model with MLLMs equipped with prompt-unaware adapters, such as MiniGPT-4 [41], mPLUG-Owl [39], BLIP-2 [21], and MLLMs that consider prompts during visual encoding, like Multimodal-GPT [43], InstructBLIP [20]. The above comparison models are zero-shot evaluation results. Second, we compare the proposed prompt-aware adapters with other popular adapters. To ensure fairness, we strive to exclude the influence of training data and the number of parameters on MLLM performance. Hence, we use the same dataset [22] to train MLLMs with MiniGPT-4/v2 [41, 12] as the uniform backbone, changing only the adapters, including linear projection, Q-Former family, cross-attention, and our prompt-aware adapter. Results are from the MME leaderboards¹

¹<https://github.com/BradyFU/Awesome-Multimodal-Large-Language-Models/tree/Evaluation>



Figure 5: Qualitative results of the proposed method on diverse perception and cognition tasks.

Tab. 2 shows the quantitative results on the COCO-QA [22] text dataset. The proposed method is capable of selectively focusing on objects mentioned in the question during visual feature extraction, leading to a noticeable improvement (approximately 5.78%) in quantity perception compared to cross-attention adapters. In the object classification, color recognition and positional reasoning tasks, our prompt-aware adapters surpass cross-attention adapters by more than 5.73%, 12.75%, and 6.95%, respectively. As depicted in Tabs 1 and 3, compared to prompt-unaware adapters, our method excels in both perception tasks (1375.02 vs 1299.79) and cognition tasks (289.28 vs 210.31) on the MME [23] benchmark.

Qualitative Results. We qualitatively compare our model with several popular MLLMs on perception and cognition tasks with more diverse visual inputs and prompts. Among the compared methods, LLaVa [11], MiniGPT-4 [41], BLIP-2 [21] adopt prompt-unaware adapters. While Flamingo [19] and InstructBLIP [20] inherently extract prompt-related visual signals through cross-attention. For visual results, refer to Figs 6~5 and Appendix. Thanks to the prompt-aware global and local attention, our model shows a clear improvement in following prompts to focus on specific visual clues.

4.3 Ablation Study

Ablation Details. In this section, we analyze the necessity of global and local attention. During validation for the former, the global text token is not added to the visual encoder for guidance, while for the latter, a simple linear projection layer is employed to replace the designed local attention component. We also test the baseline that does not incorporate any prompt-related attention mechanism during visual feature extraction. To ensure fairness, the other experimental settings are identical.

Table 2: Quantitative results of object classification, counting, color recognition, and position reasoning on the COCO-QA [22] test dataset. Evaluation metric is accuracy (%). *: frozen parameters, \checkmark : fine-tuned parameters. The best results are highlighted in bold.

Method	Object	Count	Color	Position	Total
MiniGPT-4 [41]	73.69	36.01	63.32	57.23	68.42
Linear \checkmark	74.86	62.15	69.87	63.97	72.44
Q-Former* + Linear \checkmark	56.50	43.04	29.75	35.23	49.73
Q-Former \checkmark + Linear \checkmark	28.46	38.83	32.09	26.43	29.67
Cross-Attention \checkmark	76.47	71.79	69.95	65.98	74.39
Ours	81.12	76.19	80.17	70.70	79.95

Table 3: Quantitative results of four cognition tasks on the MME [23] benchmark. Evaluation metric is scores for correct answers, with higher scores indicating better performance. *: frozen, \checkmark : fine-tuned.

Method	Common	Calculate	Translate	Code	Total
MiniGPT-4 [41]	<u>59.29</u>	45.00	0.00	40.00	144.29
Linear \checkmark	58.57	42.50	5.00	47.50	153.57
Q-Former* + Linear \checkmark	37.24	78.07	50.00	45.00	210.31
Q-Former \checkmark + Linear \checkmark	38.45	0.00	47.50	5.00	90.95
Cross-Attention \checkmark	40.00	<u>52.50</u>	15.00	57.50	165.00
Ours	99.28	50.00	87.50	<u>52.50</u>	289.28

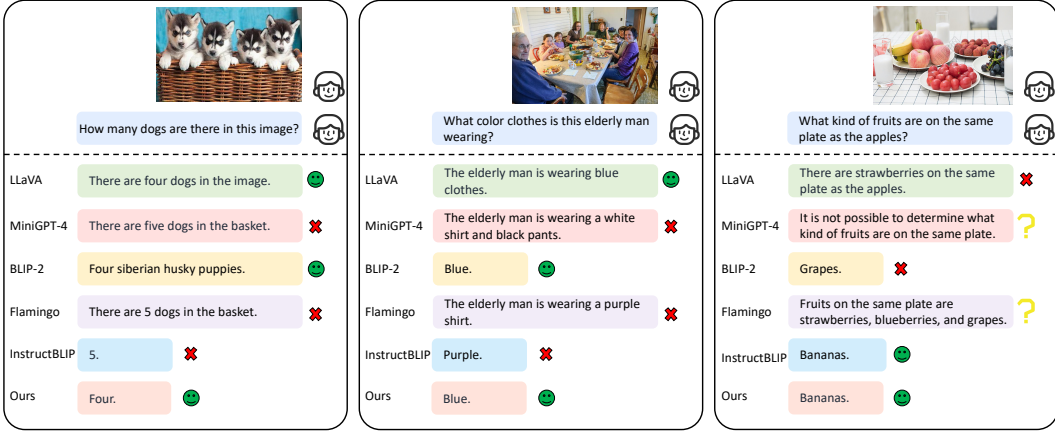


Figure 6: Comparison of qualitative results between our method and other popular MLLMs.

Table 4: Ablation study of prompt-aware global and local attention on MME [23] perception tasks. The best and second-best scores are highlighted in bold and underlined, respectively.

Method	Existence	Count	Position	Color	Posters	Celebrity	Scene	Landmark	Artwork	OCR	Total
prompt-unaware	88.33	35.00	20.00	43.33	24.82	93.82	74.75	108.75	41.50	27.5	557.82
w/o global-atten	<u>175.00</u>	<u>126.66</u>	<u>91.66</u>	<u>90.00</u>	<u>152.04</u>	129.11	147.25	117.50	<u>122.75</u>	132.50	<u>1284.49</u>
w/o local-atten	<u>175.00</u>	113.33	68.33	99.99	152.38	<u>131.17</u>	<u>155.25</u>	<u>119.75</u>	<u>122.75</u>	<u>80.00</u>	1217.97
w/ global + local	185.00	135.00	99.99	99.99	144.89	141.47	159.00	145.15	132.00	132.50	1375.02

Table 5: Ablations on COCO-QA [22] test set.

Method	Object	Count	Color	Position	Total
prompt-unaware	74.86	62.15	69.87	63.97	72.44
w/o global-atten	<u>78.67</u>	73.94	<u>79.12</u>	68.40	<u>77.75</u>
w/o local-atten	<u>77.08</u>	<u>74.59</u>	76.06	67.83	76.15
w/ global + local	81.12	76.19	80.17	70.70	79.95

Table 6: Ablations on MME [23] cognition tasks.

Method	Comm.	Cal.	Trans.	Code	Total
prompt-unaware	58.57	42.50	5.00	47.50	153.57
w/o global-atten	<u>96.42</u>	50.00	<u>55.00</u>	55.00	256.42
w/o local-atten	99.28	<u>47.50</u>	50.00	<u>52.50</u>	249.28
w/ global + local	99.28	50.00	87.50	<u>52.50</u>	289.28

Prompt-Aware Global Attention. Results (see Tab.s 4~6) suggest that the prompt-unaware method struggles to perceive visual inputs and make reasonable inferences, as it does not focus on visual signals emphasized by prompts. The global attention component directs attention allocation with complete prompt embeddings in the initial phase, thus extracting semantically aligned visual embeddings. Without prompt-aware global attention, the answer accuracy of MLLM drops obviously.

Prompt-Aware Local Attention. We evaluate the local prompt-aware adapter against linear projection without local attention. According to the results in Tab.s 4~6, the local prompt-aware attention component effectively contributes to the perceptual and cognitive capabilities of our MLLM. Especially in counting and position reasoning tasks, the correct scores are enhanced by 16.05% and 31.66% (shown in Tab. 4), respectively. Responding to fine-grained prompt guidance during the visual translation process relieves the comprehension load of LLMs.

5 Conclusions

In this paper, we introduce novel prompt-aware adapters designed to adaptively embed visual inputs based on the given prompt. Our method aims to extract the most informative visual clues relevant to the prompt, thereby enhancing the visual understanding capabilities of LLMs. We first present a global attention mechanism that utilizes a global text token for coarse-grained visual guidance. Then, we introduce a local attention mechanism that leverages local textual features to extract highly relevant visual clues with fine granularity. The resulting prompt-aware global and local visual tokens significantly reduce the visual perception burden on LLMs. Experimental results show that our method achieves competitive accuracy on multiple visual perception and cognitive tasks. We discuss the limitations and broader impacts of our method in Appendix.

References

- [1] Tom Brown, Benjamin Mann, Nick Ryder, Melanie Subbiah, Jared D Kaplan, Prafulla Dhariwal, Arvind Neelakantan, Pranav Shyam, Girish Sastry, Amanda Askell, et al. Language models are few-shot learners. *Advances in neural information processing systems*, 33:1877–1901, 2020.
- [2] Hyung Won Chung, Le Hou, Shayne Longpre, Barret Zoph, Yi Tay, William Fedus, Eric Li, Xuezhi Wang, Mostafa Dehghani, Siddhartha Brahma, Albert Webson, Shixiang Shane Gu, Zhuyun Dai, Mirac Suzgun, Xinyun Chen, Aakanksha Chowdhery, Sharan Narang, Gaurav Mishra, Adams Yu, Vincent Y. Zhao, Yanping Huang, Andrew M. Dai, Hongkun Yu, Slav Petrov, Ed H. Chi, Jeff Dean, Jacob Devlin, Adam Roberts, Denny Zhou, Quoc V. Le, and Jason Wei. Scaling instruction-finetuned language models. *CoRR*, abs/2210.11416:1–12, 2022.
- [3] OpenAI. Introducing chatgpt, 2023. <https://openai.com/blog/chatgpt>.
- [4] Hugo Touvron, Thibaut Lavril, Gautier Izacard, Xavier Martinet, Marie-Anne Lachaux, Timothée Lacroix, Baptiste Rozière, Naman Goyal, Eric Hambro, Faisal Azhar, et al. Llama: Open and efficient foundation language models. *arXiv preprint arXiv:2302.13971*, abs/2302.13971:1–12, 2023.
- [5] Wei-Lin Chiang, Zhuohan Li, Zi Lin, Ying Sheng, Zhanghao Wu, Hao Zhang, Lianmin Zheng, Siyuan Zhuang, Yonghao Zhuang, Joseph E Gonzalez, et al. Vicuna: An open-source chatbot impressing gpt-4 with 90%* chatgpt quality. See <https://vicuna.lmsys.org> (accessed 14 April 2023), 2(3):6, 2023.
- [6] Danny Driess, Fei Xia, Mehdi SM Sajjadi, Corey Lynch, Aakanksha Chowdhery, Brian Ichter, Ayzan Wahid, Jonathan Tompson, Quan Vuong, Tianhe Yu, et al. Palm-e: An embodied multimodal language model. *arXiv preprint arXiv:2303.03378*, 2023.
- [7] Zhengyuan Yang, Linjie Li, Jianfeng Wang, Kevin Lin, Ehsan Azarnasab, Faisal Ahmed, Zicheng Liu, Ce Liu, Michael Zeng, and Lijuan Wang. Mm-react: Prompting chatgpt for multimodal reasoning and action. *arXiv preprint arXiv:2303.11381*, 2023.
- [8] KunChang Li, Yanan He, Yi Wang, Yizhuo Li, Wenhai Wang, Ping Luo, Yali Wang, Limin Wang, and Yu Qiao. Videochat: Chat-centric video understanding. *arXiv preprint arXiv:2305.06355*, 2023.
- [9] Sivan Doveh, Assaf Arbelle, Sivan Harary, Roei Herzig, Donghyun Kim, Paola Cascante-Bonilla, Amit Alfassy, Rameswar Panda, Raja Giryes, Rogerio Feris, et al. Dense and aligned captions (dac) promote compositional reasoning in vl models. *Advances in Neural Information Processing Systems*, 36, 2024.
- [10] Zhiliang Peng, Wenhui Wang, Li Dong, Yaru Hao, Shaohan Huang, Shuming Ma, and Furu Wei. Kosmos-2: Grounding multimodal large language models to the world. *arXiv preprint arXiv:2306.14824*, 2023.
- [11] Haotian Liu, Chunyuan Li, Qingyang Wu, and Yong Jae Lee. Visual instruction tuning. *arXiv preprint arXiv:2304.08485*, 2023.
- [12] Jun Chen, Deyao Zhu, Xiaoqian Shen, Xiang Li, Zechun Liu, Pengchuan Zhang, Raghuraman Krishnamoorthi, Vikas Chandra, Yunyang Xiong, and Mohamed Elhoseiny. Minigpt-v2: large language model as a unified interface for vision-language multi-task learning. *arXiv preprint arXiv:2310.09478*, 2023.
- [13] Keqin Chen, Zhao Zhang, Weili Zeng, Richong Zhang, Feng Zhu, and Rui Zhao. Shikra: Unleashing multimodal llm’s referential dialogue magic. *arXiv preprint arXiv:2306.15195*, 2023.
- [14] Yan Zeng, Hanbo Zhang, Jiani Zheng, Jiangnan Xia, Guoqiang Wei, Yang Wei, Yuchen Zhang, and Tao Kong. What matters in training a gpt4-style language model with multimodal inputs? *arXiv preprint arXiv:2307.02469*, 2023.
- [15] Yixuan Su, Tian Lan, Huayang Li, Jialu Xu, Yan Wang, and Deng Cai. Pandagpt: One model to instruction-follow them all. *arXiv preprint arXiv:2305.16355*, 2023.
- [16] Qiang Zhou, Zhibin Wang, Wei Chu, Yinghui Xu, Hao Li, and Yuan Qi. Infmllm: A unified framework for visual-language tasks. *arXiv preprint arXiv:2311.06791*, 2023.
- [17] Junbum Cha, Wooyoung Kang, Jonghwan Mun, and Byungseok Roh. Honeybee: Locality-enhanced projector for multimodal llm. *arXiv preprint arXiv:2312.06742*, 2023.
- [18] Wenhai Wang, Zhe Chen, Xiaokang Chen, Jiannan Wu, Xizhou Zhu, Gang Zeng, Ping Luo, Tong Lu, Jie Zhou, Yu Qiao, et al. Visionllm: Large language model is also an open-ended decoder for vision-centric tasks. *Advances in Neural Information Processing Systems*, 36:1–13, 2024.
- [19] Jean-Baptiste Alayrac, Jeff Donahue, Pauline Luc, Antoine Miech, Iain Barr, Yana Hasson, Karel Lenc, Arthur Mensch, Katherine Millican, Malcolm Reynolds, et al. Flamingo: a visual language model for few-shot learning. *Advances in Neural Information Processing Systems*, 35:23716–23736, 2022.
- [20] Wenliang Dai, Junnan Li, Dongxu Li, Anthony Meng Huat Tiong, Junqi Zhao, Weisheng Wang, Boyang Li, Pascale N Fung, and Steven Hoi. Instructblip: Towards general-purpose vision-language models with instruction tuning. *Advances in Neural Information Processing Systems*, 36, 2024.
- [21] Junnan Li, Dongxu Li, Silvio Savarese, and Steven Hoi. Blip-2: Bootstrapping language-image pre-training with frozen image encoders and large language models. *arXiv preprint arXiv:2301.12597*, 2023.

- [22] Mengye Ren, Ryan Kiros, and Richard Zemel. Exploring models and data for image question answering. *Advances in neural information processing systems*, 28, 2015.
- [23] Chaoyou Fu, Peixian Chen, Yunhang Shen, Yulei Qin, Mengdan Zhang, Xu Lin, Zhenyu Qiu, Wei Lin, Jinrui Yang, Xiawu Zheng, et al. Mme: A comprehensive evaluation benchmark for multimodal large language models. *arXiv preprint arXiv:2306.13394*, abs/2306.13394:1–12, 2023.
- [24] Alexander Kirillov, Eric Mintun, Nikhila Ravi, Hanzi Mao, Chloé Rolland, Laura Gustafson, Tete Xiao, Spencer Whitehead, Alexander C. Berg, Wan-Yen Lo, Piotr Dollár, and Ross B. Girshick. Segment anything. In *IEEE/CVF International Conference on Computer Vision, ICCV 2023, October 1-6, 2023*, pages 3992–4003, Paris, France, 2023. IEEE.
- [25] Ron Mokady, Amir Hertz, and Amit H Bermano. Clipcap: Clip prefix for image captioning. *arXiv preprint arXiv:2111.09734*, 2021.
- [26] Maxime Oquab, Timothée Darcet, Théo Moutakanni, Huy Vo, Marc Szafraniec, Vasil Khalidov, Pierre Fernandez, Daniel Haziza, Francisco Massa, Alaaeldin El-Nouby, et al. Dinov2: Learning robust visual features without supervision. *arXiv preprint arXiv:2304.07193*, 2023.
- [27] Alec Radford, Jong Wook Kim, Chris Hallacy, Aditya Ramesh, Gabriel Goh, Sandhini Agarwal, Girish Sastry, Amanda Askell, Pamela Mishkin, Jack Clark, et al. Learning transferable visual models from natural language supervision. In *International conference on machine learning*, pages 8748–8763. PMLR, 2021.
- [28] Long Ouyang, Jeffrey Wu, Xu Jiang, Diogo Almeida, Carroll Wainwright, Pamela Mishkin, Chong Zhang, Sandhini Agarwal, Katarina Slama, Alex Ray, et al. Training language models to follow instructions with human feedback. *Advances in Neural Information Processing Systems*, 35:27730–27744, 2022.
- [29] Aakanksha Chowdhery, Sharan Narang, Jacob Devlin, Maarten Bosma, Gaurav Mishra, Adam Roberts, Paul Barham, Hyung Won Chung, Charles Sutton, Sebastian Gehrmann, et al. Palm: Scaling language modeling with pathways. *Journal of Machine Learning Research*, 24(240):1–113, 2023.
- [30] Romal Thoppilan, Daniel De Freitas, Jamie Hall, Noam Shazeer, Apoorv Kulshreshtha, Heng-Tze Cheng, Alicia Jin, Taylor Bos, Leslie Baker, Yu Du, et al. Lamda: Language models for dialog applications. *arXiv preprint arXiv:2201.08239*, 2022.
- [31] Susan Zhang, Stephen Roller, Naman Goyal, Mikel Artetxe, Moya Chen, Shuohui Chen, Christopher Dewan, Mona Diab, Xian Li, Xi Victoria Lin, et al. Opt: Open pre-trained transformer language models. *arXiv preprint arXiv:2205.01068*, abs/2205.01068:1–12, 2022.
- [32] Zongxin Yang, Guikun Chen, Xiaodi Li, Wenguan Wang, and Yi Yang. Doraemongpt: Toward understanding dynamic scenes with large language models (exemplified as a video agent). In *ICML*, 2024.
- [33] Shengding Hu, Yuge Tu, Xu Han, Chaoqun He, Ganqu Cui, Xiang Long, Zhi Zheng, Yewei Fang, Yuxiang Huang, Weilin Zhao, et al. Minicpm: Unveiling the potential of small language models with scalable training strategies. *arXiv preprint arXiv:2404.06395*, 2024.
- [34] Lin Chen, Jisong Li, Xiaoyi Dong, Pan Zhang, Conghui He, Jiaqi Wang, Feng Zhao, and Dahua Lin. Sharegpt4v: Improving large multi-modal models with better captions. *arXiv preprint arXiv:2311.12793*, 2023.
- [35] Kecheng Zheng, Yifei Zhang, Wei Wu, Fan Lu, Shuailei Ma, Xin Jin, Wei Chen, and Yujun Shen. Dreamlip: Language-image pre-training with long captions. *arXiv preprint arXiv:2403.17007*, 2024.
- [36] Yanwei Li, Yuechen Zhang, Chengyao Wang, Zhisheng Zhong, Yixin Chen, Ruihang Chu, Shaoteng Liu, and Jiaya Jia. Mini-gemini: Mining the potential of multi-modality vision language models. *arXiv preprint arXiv:2403.18814*, 2024.
- [37] Wei Li, Hehe Fan, Yongkang Wong, Yi Yang, and Mohan Kankanhalli. Improve context understanding in multimodal large language models via multimodal composition learning. In *ICML*, 2024.
- [38] Jinze Bai, Shuai Bai, Shusheng Yang, Shijie Wang, Sinan Tan, Peng Wang, Junyang Lin, Chang Zhou, and Jingren Zhou. Qwen-vl: A versatile vision-language model for understanding, localization, text reading, and beyond. 2023.
- [39] Qinghao Ye, Haiyang Xu, Guohai Xu, Jiabo Ye, Ming Yan, Yiyang Zhou, Junyang Wang, Anwen Hu, Pengcheng Shi, Yaya Shi, et al. mplug-owl: Modularization empowers large language models with multimodality. *arXiv preprint arXiv:2304.14178*, 2023.
- [40] Andrew Jaegle, Felix Gimeno, Andy Brock, Oriol Vinyals, Andrew Zisserman, and Joao Carreira. Perceiver: General perception with iterative attention. In *International conference on machine learning*, pages 4651–4664. PMLR, 2021.
- [41] Deyao Zhu, Jun Chen, Xiaoqian Shen, Xiang Li, and Mohamed Elhoseiny. Minigpt-4: Enhancing vision-language understanding with advanced large language models. *arXiv preprint arXiv:2304.10592*, 2023.

- [42] Tianyu Yu, Jinyi Hu, Yuan Yao, Haoye Zhang, Yue Zhao, Chongyi Wang, Shan Wang, Yinxi Pan, Jiao Xue, Dahai Li, et al. Reformulating vision-language foundation models and datasets towards universal multimodal assistants. *arXiv preprint arXiv:2310.00653*, 2023.
- [43] Tao Gong, Chengqi Lyu, Shilong Zhang, Yudong Wang, Miao Zheng, Qian Zhao, Kuikun Liu, Wenwei Zhang, Ping Luo, and Kai Chen. Multimodal-gpt: A vision and language model for dialogue with humans. *arXiv preprint arXiv:2305.04790*, 2023.
- [44] Bo Li, Yuanhan Zhang, Liangyu Chen, Jinghao Wang, Jingkang Yang, and Ziwei Liu. Otter: A multi-modal model with in-context instruction tuning, 2023.
- [45] Juncheng Li, Kaihang Pan, Zhiqi Ge, Minghe Gao, Wei Ji, Wenqiao Zhang, Tat-Seng Chua, Siliang Tang, Hanwang Zhang, and Yueting Zhuang. Fine-tuning multimodal llms to follow zero-shot demonstrative instructions. In *The Twelfth International Conference on Learning Representations*, 2023.
- [46] Dzmitry Bahdanau, Kyunghyun Cho, and Yoshua Bengio. Neural machine translation by jointly learning to align and translate. In Yoshua Bengio and Yann LeCun, editors, *3rd International Conference on Learning Representations, ICLR 2015, San Diego, CA, USA, May 7-9, 2015, Conference Track Proceedings*, 2015.
- [47] Siyu Lu, Mingzhe Liu, Lirong Yin, Zhengtong Yin, Xuan Liu, and Wenfeng Zheng. The multi-modal fusion in visual question answering: a review of attention mechanisms. *PeerJ Computer Science*, 9:e1400, 2023.
- [48] Dehua Zheng, Wenhui Dong, Hailin Hu, Xinghao Chen, and Yunhe Wang. Less is more: Focus attention for efficient detr. In *Proceedings of the IEEE/CVF International Conference on Computer Vision*, pages 6674–6683, 2023.
- [49] Man Yao, Guangshe Zhao, Hengyu Zhang, Yifan Hu, Lei Deng, Yonghong Tian, Bo Xu, and Guoqi Li. Attention spiking neural networks. *IEEE transactions on pattern analysis and machine intelligence*, 2023.
- [50] Kelvin Xu, Jimmy Ba, Ryan Kiros, Kyunghyun Cho, Aaron Courville, Ruslan Salakhudinov, Rich Zemel, and Yoshua Bengio. Show, attend and tell: Neural image caption generation with visual attention. In *International conference on machine learning*, pages 2048–2057. PMLR, 2015.
- [51] Jiasen Lu, Jianwei Yang, Dhruv Batra, and Devi Parikh. Hierarchical question-image co-attention for visual question answering. *Advances in neural information processing systems*, 29, 2016.
- [52] Zichao Yang, Diyi Yang, Chris Dyer, Xiaodong He, Alex Smola, and Eduard Hovy. Hierarchical attention networks for document classification. In *Proceedings of the 2016 conference of the North American chapter of the association for computational linguistics: human language technologies*, pages 1480–1489, 2016.
- [53] Zhouhan Lin, Minwei Feng, Cicero Nogueira dos Santos, Mo Yu, Bing Xiang, Bowen Zhou, and Yoshua Bengio. A structured self-attentive sentence embedding. *arXiv preprint arXiv:1703.03130*, 2017.
- [54] Tim Rocktäschel, Johannes Welbl, and Sebastian Riedel. Frustratingly short attention spans in neural language modeling, 2017.
- [55] Ashish Vaswani, Noam Shazeer, Niki Parmar, Jakob Uszkoreit, Llion Jones, Aidan N Gomez, Łukasz Kaiser, and Illia Polosukhin. Attention is all you need. *Advances in neural information processing systems*, 30, 2017.
- [56] Xi Wei, Tianzhu Zhang, Yan Li, Yongdong Zhang, and Feng Wu. Multi-modality cross attention network for image and sentence matching. In *Proceedings of the IEEE/CVF conference on computer vision and pattern recognition*, pages 10941–10950, 2020.
- [57] Hugo Touvron, Louis Martin, Kevin Stone, Peter Albert, Amjad Almahairi, Yasmine Babaei, Nikolay Bashlykov, Soumya Batra, Prajjwal Bhargava, Shruti Bhosale, et al. Llama 2: Open foundation and fine-tuned chat models. *arXiv preprint arXiv:2307.09288*, 2023.
- [58] Yuxin Fang, Wen Wang, Binhui Xie, Quan Sun, Ledell Wu, Xinggang Wang, Tiejun Huang, Xinlong Wang, and Yue Cao. Eva: Exploring the limits of masked visual representation learning at scale. In *Proceedings of the IEEE/CVF Conference on Computer Vision and Pattern Recognition*, pages 19358–19369, BC, Canada, 2023. IEEE.
- [59] Ilya Loshchilov and Frank Hutter. Decoupled weight decay regularization. *arXiv preprint arXiv:1711.05101*, 2017.
- [60] Christoph Schuhmann, Richard Vencu, Romain Beaumont, Robert Kaczmarczyk, Clayton Mullis, Aarush Katta, Theo Coombes, Jenia Jitsev, and Aran Komatsuzaki. Laion-400m: Open dataset of clip-filtered 400 million image-text pairs. *arXiv preprint arXiv:2111.02114*, 2021.
- [61] Piyush Sharma, Nan Ding, Sebastian Goodman, and Radu Soricut. Conceptual captions: A cleaned, hypernymed, image alt-text dataset for automatic image captioning. In *Proceedings of the 56th Annual Meeting of the Association for Computational Linguistics (Volume 1: Long Papers)*, pages 2556–2565, 2018.

- [62] Vicente Ordonez, Girish Kulkarni, and Tamara Berg. Im2text: Describing images using 1 million captioned photographs. *Advances in neural information processing systems*, 24, 2011.
- [63] Tsung-Yi Lin, Michael Maire, Serge Belongie, James Hays, Pietro Perona, Deva Ramanan, Piotr Dollár, and C Lawrence Zitnick. Microsoft coco: Common objects in context. In *Computer Vision—ECCV 2014: 13th European Conference, Zurich, Switzerland, September 6–12, 2014, Proceedings, Part V 13*, pages 740–755. Springer, 2014.
- [64] Oleksii Sidorov, Ronghang Hu, Marcus Rohrbach, and Amanpreet Singh. Textcaps: a dataset for image captioning with reading comprehension. In *Computer Vision—ECCV 2020: 16th European Conference, Glasgow, UK, August 23–28, 2020, Proceedings, Part II 16*, pages 742–758. Springer, 2020.
- [65] Sahar Kazemzadeh, Vicente Ordonez, Mark Matten, and Tamara Berg. Referitgame: Referring to objects in photographs of natural scenes. In *Proceedings of the 2014 conference on empirical methods in natural language processing (EMNLP)*, pages 787–798, 2014.
- [66] Licheng Yu, Patrick Poirson, Shan Yang, Alexander C Berg, and Tamara L Berg. Modeling context in referring expressions. In *Computer Vision—ECCV 2016: 14th European Conference, Amsterdam, The Netherlands, October 11–14, 2016, Proceedings, Part II 14*, pages 69–85. Springer, 2016.
- [67] Junhua Mao, Jonathan Huang, Alexander Toshev, Oana Camburu, Alan L Yuille, and Kevin Murphy. Generation and comprehension of unambiguous object descriptions. In *Proceedings of the IEEE conference on computer vision and pattern recognition*, pages 11–20, 2016.
- [68] Drew A Hudson and Christopher D Manning. Gqa: A new dataset for real-world visual reasoning and compositional question answering. In *Proceedings of the IEEE/CVF conference on computer vision and pattern recognition*, pages 6700–6709, 2019.
- [69] Yash Goyal, Tejas Khot, Douglas Summers-Stay, Dhruv Batra, and Devi Parikh. Making the v in vqa matter: Elevating the role of image understanding in visual question answering. In *Proceedings of the IEEE conference on computer vision and pattern recognition*, pages 6904–6913, 2017.
- [70] Anand Mishra, Shashank Shekhar, Ajeet Kumar Singh, and Anirban Chakraborty. Ocr-vqa: Visual question answering by reading text in images. In *2019 international conference on document analysis and recognition (ICDAR)*, pages 947–952. IEEE, 2019.
- [71] Kenneth Marino, Mohammad Rastegari, Ali Farhadi, and Roozbeh Mottaghi. Ok-vqa: A visual question answering benchmark requiring external knowledge. In *Proceedings of the IEEE/cvf conference on computer vision and pattern recognition*, pages 3195–3204, 2019.
- [72] Dustin Schwenk, Apoorv Khandelwal, Christopher Clark, Kenneth Marino, and Roozbeh Mottaghi. A-okvqa: A benchmark for visual question answering using world knowledge. In *European Conference on Computer Vision*, pages 146–162. Springer, 2022.
- [73] Bryan A Plummer, Liwei Wang, Chris M Cervantes, Juan C Caicedo, Julia Hockenmaier, and Svetlana Lazebnik. Flickr30k entities: Collecting region-to-phrase correspondences for richer image-to-sentence models. In *Proceedings of the IEEE international conference on computer vision*, pages 2641–2649, 2015.
- [74] Renrui Zhang, Jiaming Han, Aojun Zhou, Xiangfei Hu, Shilin Yan, Pan Lu, Hongsheng Li, Peng Gao, and Yu Qiao. Llama-adapter: Efficient fine-tuning of language models with zero-init attention. *arXiv preprint arXiv:2303.16199*, abs/2303.16199:1–12, 2023.
- [75] Ao Zhang, Hao Fei, Yuan Yao, Wei Ji, Li Li, Zhiyuan Liu, and Tat-Seng Chua. Vpqrans: Transfer visual prompt generator across llms. *Advances in Neural Information Processing Systems*, 36, 2024.
- [76] Gen Luo, Yiyi Zhou, Tianhe Ren, Shengxin Chen, Xiaoshuai Sun, and Rongrong Ji. Cheap and quick: Efficient vision-language instruction tuning for large language models. *Advances in Neural Information Processing Systems*, 36, 2024.
- [77] Fuxiao Liu, Kevin Lin, Linjie Li, Jianfeng Wang, Yaser Yacoob, and Lijuan Wang. Mitigating hallucination in large multi-modal models via robust instruction tuning. In *The Twelfth International Conference on Learning Representations*, 2023.
- [78] Qingqiu Huang, Yu Xiong, Anyi Rao, Jiase Wang, and Dahua Lin. Movienet: A holistic dataset for movie understanding. *CoRR*, abs/2007.10937, 2020.
- [79] Hui Mao, Ming Cheung, and James She. Deepart: Learning joint representations of visual arts. In Qiong Liu, Rainer Lienhart, Haohong Wang, Sheng-Wei "Kuan-Ta" Chen, Susanne Boll, Yi-Ping Phoebe Chen, Gerald Friedland, Jia Li, and Shuicheng Yan, editors, *Proceedings of the 2017 ACM on Multimedia Conference, MM 2017, Mountain View, CA, USA, October 23–27, 2017*, pages 1183–1191. ACM, 2017.
- [80] Hui Mao, James She, and Ming Cheung. Visual arts search on mobile devices. *ACM Trans. Multim. Comput. Commun. Appl.*, 15(2s):60:1–60:23, 2019.

- [81] Tobias Weyand, André Araújo, Bingyi Cao, and Jack Sim. Google landmarks dataset v2 - A large-scale benchmark for instance-level recognition and retrieval. In *2020 IEEE/CVF Conference on Computer Vision and Pattern Recognition, CVPR 2020, Seattle, WA, USA, June 13-19, 2020*, pages 2572–2581. Computer Vision Foundation / IEEE, 2020.
- [82] Bolei Zhou, Àgata Lapedriza, Jianxiong Xiao, Antonio Torralba, and Aude Oliva. Learning deep features for scene recognition using places database. In Zoubin Ghahramani, Max Welling, Corinna Cortes, Neil D. Lawrence, and Kilian Q. Weinberger, editors, *Advances in Neural Information Processing Systems 27: Annual Conference on Neural Information Processing Systems 2014, December 8-13 2014, Montreal, Quebec, Canada*, pages 487–495, 2014.
- [83] Yuliang Liu, Lianwen Jin, Shuaitao Zhang, Canjie Luo, and Sheng Zhang. Curved scene text detection via transverse and longitudinal sequence connection. *Pattern Recognit.*, 90:337–345, 2019.

A Appendix Overview

In summary, the appendix is organized as follows:

Appendix B: Additional experiments and analysis.

Appendix C: More visualization results of prompt-aware global and local attention.

Appendix D: More qualitative results and analysis.

Appendix E: More details of COCO-QA dataset and MME benchmark.

Appendix F: Prompts used for fine-tuning.

B Additional Experiments and Analysis

B.1 Comparison of Text Encoders

During the implementation of the global and local attention mechanisms, we compare the quantitative results of text feature extraction by different text encoders. Tab.s 7~9 show comparison results of adopting CLIP [27] and Llama 2 [4] to extract prompt features for global and local attention. G-Num refers to the number of text tokens used in global attention. 0 means no global attention is used in the model architecture, 1 means only one global text token is used, and L means the total number of text tokens.

The experimental results show that using global text tokens performs better than not using them, confirming the effectiveness of our prompt-aware global attention. Besides, CLIP [27] generally performs better than Llama 2 [4] on perceptual tasks, while Llama 2 [4] excels in cognitive tasks. This may be because, in perceptual tasks, the text features extracted by CLIP can better align with visual features. In cognitive tasks, Llama 2 [4], having been trained on vast amounts of data, possesses superior reasoning abilities.

Table 7: Comparison results of using different text encoders (CLIP [27] and Llama 2 [4]) to extract prompt features for global and local attention. G-Num refers to the number of text tokens used in global attention, and L is the total amount of text tokens. The evaluation is built on the MME [23] perception tasks, the evaluation metric is correct answer scores, with higher scores being better. The best and second-best scores are highlighted in bold and underlined, respectively.

Method			Perception Tasks										
G-Num	Global	Local	Existence	Count	Position	Color	Poster	Celebrity	Scene	Landmark	Artwork	OCR	Total
0	-	-	88.33	35.00	20.00	43.33	24.82	93.82	74.75	108.75	41.50	27.5	557.82
0	-	CLIP	<u>175.00</u>	<u>126.66</u>	<u>91.66</u>	90.00	<u>152.04</u>	129.11	147.25	117.50	<u>122.75</u>	132.50	<u>1284.49</u>
1	CLIP	-	<u>175.00</u>	113.33	68.33	99.99	152.38	131.17	155.25	119.75	<u>122.75</u>	80.00	1217.97
1	CLIP	Llama 2	170.00	121.66	48.33	99.99	130.27	127.94	149.50	134.25	119.50	<u>125.00</u>	1226.46
L	CLIP	Llama 2	170.00	106.66	48.33	70.00	128.23	118.23	154.25	139.50	119.25	102.50	1156.96
L	CLIP	CLIP	160.0	111.66	73.33	90.00	133.33	<u>131.76</u>	<u>158.00</u>	146.50	119.25	95.00	1218.84
1	CLIP	CLIP	185.00	135.00	99.99	99.99	144.89	141.47	159.00	<u>145.15</u>	132.00	132.50	1375.02

Table 8: Comparison results of using different text encoders (CLIP [27] and Llama 2 [4]) to extract prompt features for global and local attention. G-Num refers to the number of text tokens used in global attention, and L is the total amount of text tokens. The evaluation is built on the MME [23] cognition tasks, the evaluation metric is correct answer scores, with higher scores being better. The best and second-best scores are highlighted in bold and underlined, respectively.

Method			Cognition Tasks				
G-Num	Global	Local	Common Sense	Calculation	Translation	Code	Total
0	-	-	58.57	42.50	5.00	47.50	153.57
0	-	CLIP	<u>96.42</u>	<u>50.00</u>	55.00	55.00	<u>256.42</u>
1	CLIP	-	99.28	47.50	50.00	<u>52.50</u>	249.28
1	CLIP	Llama 2	83.57	57.50	57.50	47.50	246.07
L	CLIP	Llama 2	92.14	<u>50.00</u>	<u>65.00</u>	47.50	254.64
L	CLIP	CLIP	<u>96.42</u>	45.00	57.50	47.50	246.42
1	CLIP	CLIP	99.28	<u>50.00</u>	87.50	<u>52.50</u>	289.28

Table 9: Comparison results of using different text encoders (CLIP [27] and Llama 2 [4]) to extract prompt features for global and local attention. G-Num refers to the number of text tokens used in global attention, and L is the total amount of text tokens. The evaluation is built on the COCO-QA [22] cognition tasks, the evaluation metric is correct answer scores, with higher scores being better. The best and second-best scores are highlighted in bold and underlined, respectively.

Method			Perception Tasks				
G-Num	Global	Local	Object	Count	Color	Position	Total
0	-	-	74.86	62.15	69.87	63.97	72.44
0	-	CLIP	78.67	73.94	<u>79.12</u>	68.40	77.75
1	CLIP	-	77.08	74.59	76.06	67.83	76.15
1	CLIP	Llama 2	<u>80.57</u>	76.13	78.64	68.76	79.25
L	CLIP	Llama 2	80.41	76.62	77.41	70.94	79.07
L	CLIP	CLIP	80.51	<u>76.40</u>	79.07	69.00	79.25
1	CLIP	CLIP	81.12	76.19	80.17	<u>70.70</u>	79.95

Table 10: Comparison results of using different *Ratio* to combine global and local visual features. The value range of *Ratio* is 0-1. The evaluation is built on the MME [23] perception tasks, the evaluation metric is correct answer scores, with higher scores being better. The best and second-best scores are highlighted in bold and underlined, respectively.

<i>Ratio</i>	Existence	Count	Position	Color	Posters	Celebrity	Scene	Landmark	Artwork	OCR	Total
0.2	85.00	65.00	58.33	51.66	71.42	40.29	52.25	99.75	56.25	70.00	649.97
0.4	175.00	108.33	68.33	73.33	130.27	136.17	<u>156.75</u>	148.25	<u>136.00</u>	<u>95.00</u>	1227.44
0.6	175.00	126.66	<u>91.66</u>	90.00	<u>152.04</u>	129.11	147.25	117.50	122.75	132.50	1284.49
0.8	<u>185.00</u>	135.00	99.99	<u>99.99</u>	144.89	141.47	159.00	<u>145.15</u>	132.00	132.50	1375.02
1.0	190.0	<u>128.33</u>	<u>91.66</u>	150.00	152.72	144.41	155.50	141.00	139.75	80.00	<u>1373.38</u>

Table 11: Comparison results of using different *Ratio* to combine global and local visual features. The value range of *Ratio* is 0-1. The evaluation is built on the MME [23] cognition tasks. The evaluation metric is correct answer scores, with higher scores being better. The best and second-best scores are highlighted in bold and underlined, respectively.

<i>Ratio</i>	Commonsense	Calculation	Translation	Code	Total
0.2	67.14	65.00	5.00	<u>47.50</u>	184.64
0.4	<u>97.14</u>	47.50	50.00	<u>47.50</u>	242.14
0.6	96.42	50.00	55.00	55.00	256.42
0.8	92.85	<u>57.50</u>	<u>57.50</u>	45.00	252.85
1.0	103.57	55.00	72.50	<u>47.50</u>	278.57

B.2 Residual Visual Details

We also try to fuse the visual features obtained through global attention and the visual features obtained through local attention. *Ratio* represents the retention ratio of local visual features, and the retention ratio of global visual features is $(1 - Ratio)$. For example, when $Ratio=0.2$, it means that the local features are multiplied by 0.2 and the global features are multiplied by 0.8 and then added.

Tab.s 10~11 show the impact of using different *Ratio* values on the model’s perceptual and cognitive tasks. Experimental results show that the weighted sum of global and local features helps to improve model performance to a certain extent but not very much. In addition, when local features account for greater weight, the model seems to perform better.

B.3 Exploration of Prompt-Aware Q-Former

Inspired by InstructBLIP [21], we further explore novel architectures for prompt-aware Q-Former. In this section, we implement a Q-Former-based prompt-aware adapter. Specifically, we try to add prompt cross-attention to different blocks in Q-Former. Table 12 shows the quantitative evaluation results of various model-specific implementations. Through extensive experiments, we found that the Q-former is difficult to train, and it tends to lose previously learned knowledge when fine-tuning on downstream tasks. Additionally, the effects of injecting text features into different layers of the Q-Former vary significantly.

Table 12: Quantitative evaluation results of various model-specific implementations. The “No.” is the number of the experimental setup. The “BlockNum” denotes the number of attention blocks in which the text cross-attention layer is inserted. The “OC”, “CON”, “CR”, and “PR” represent the four tasks of object classification, counting, color recognition, and position reasoning, respectively. The “Acc (%)” denotes accuracy and “Total Acc (%)” refers to the overall accuracy on four tasks.

No.	BlockNum	OC Acc (%)	CON Acc (%)	CR Acc (%)	PR Acc (%)	Total Acc (%)
1	0	78.09	73.22	74.23	65.54	76.33
2	0+1	65.46	70.84	51.55	52.31	62.73
3	0+1+2	77.67	65.48	73.49	63.08	75.23
4	0+1+2+3	78.20	69.95	69.89	62.47	75.29
5	0+1+2+3+4	77.72	69.35	79.06	62.47	76.38
6	0+1+2+3+4+5	78.52	71.43	74.85	67.39	76.73
7	1	29.31	36.31	8.68	10.47	25.23
8	1+3+5+7+11	33.21	29.47	9.79	22.77	28.50
9	0+2+4+6+8+10	77.98	69.05	72.37	64.31	75.59
10	11	77.02	68.46	60.97	62.77	72.93
11	10+11	75.15	71.73	72.37	64.62	73.79
12	9+10+11	74.89	69.95	72.87	66.47	73.69
13	8+9+10+11	75.09	69.95	73.49	65.85	73.89
14	7+8+9+10+11	78.65	72.03	78.31	67.69	77.26
15	6+7+8+9+10+11	77.72	68.76	75.97	64.92	76.1
16	0+1+2+3+4+5+6+7+8+9+10+11	76.70	69.05	74.73	64.62	75.09

C More Visualization Results of Prompt-Aware Global and Local Attention

In this section, we present more results of global and local attention visualization. Fig. 7 aims to verify the role of the proposed attention mechanism in object recognition tasks. Figs. 8 to 10 re-validate the superiority of the proposed prompt-aware adapter in counting. Fig. 11 and Fig. 12 illustrate the focal points of the attention mechanism in color recognition and position reasoning tasks, respectively. A large number of visualization results illustrate the effectiveness of our method and provide a degree of interpretability.

D More Qualitative Results and Analysis

We also provide more qualitative results with a wider range of image and prompt inputs (as shown in Figs. 13~26). Specifically, Fig. 13 focuses on the color recognition task, Fig. 14 on the counting task, Fig. 15 on the position reasoning task, Fig. 17 on the OCR task, Fig. 18 on the landmark recognition task, Fig. 19 on the celebrity recognition task, and Fig. 20 on the poster recognition task. Additionally, Fig. 21, Fig. 22 and Fig. 23 respectively showcase the model’s capabilities in computation, coding, and common sense reasoning. Finally, Figs. 24~26 provide visualization results for mixed perception tasks.

E More Details of COCO-QA Dataset and MME Benchmark

E.1 COCO-QA Dataset

Object Classification. The primary objective of the object classification task is to accurately recognize objects in the given visual input and determine the category to which they belong. The metric used to evaluate this task is accuracy. For this task, we utilize 82,198 question-answer pairs related to objects from the COCO-QA dataset [22], with 78,666 used for fine-tuning and 3,532 for testing. The questions typically involve the use of “what” to inquire about the object type. In addition, a succinct single-word answer is employed to precisely indicate the response.

Counting. The main goal of counting is to recognize and count the number of questioned objects from the given visual input. The metric employed to assess this task is accuracy. In the counting task, we use 19,568 question-answer pairs related to the number of objects from the COCO-QA dataset [22], with 1,8761 used for fine-tuning and 807 for testing. When posing questions, the inquiry typically involves the use of “how many” to inquire about the object amount. Likewise, we only use a single word describing the quantity in the response.

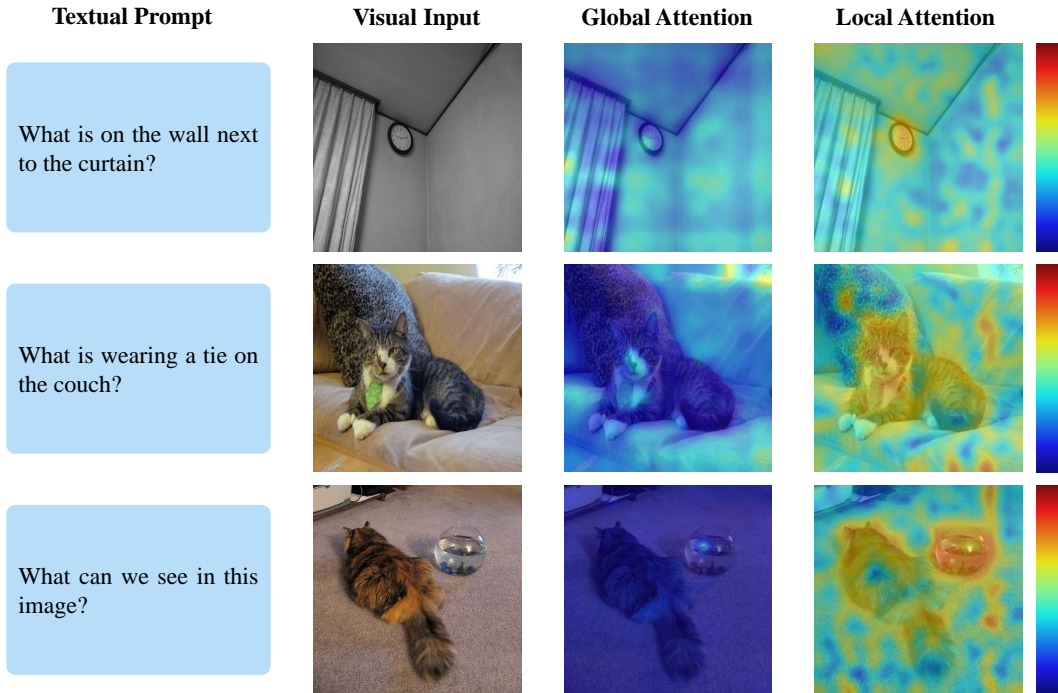


Figure 7: Visualization of prompt-aware global and local attention on the object perception task. Visualization results show that global attention spans the entire prompt content, while local attention concentrates predominantly on the specific object in question.

Color Recognition. The color recognition task is designed to detect objects in questions and perceive color information from the input visual signal. The metric employed to assess this task is also accuracy. In this task, we utilize 8,640 question-answer pairs related to objects from the COCO-QA dataset [22], with 8,304 used for fine-tuning and 336 for testing. Questions related to color are relatively straightforward, usually beginning with “What is the color of”. To facilitate quantitative evaluation, responses are kept as brief as possible for color-related words.

Position Reasoning. In the position reasoning task, our primary goal is to infer the location information of the queried object based on the input visual content. Similarly, we adopt the accuracy as the evaluation metric. We adopt 7,278 question-answer pairs related to objects from the COCO-QA dataset [22], with 6,953 used for fine-tuning and 325 for testing. In this task, questions are formatted to start with “where” to ask for the position of an object. Answers mostly be places, scenes, or large objects that contain smaller objects.

Examples of questions and answers from four perceptual tasks are shown in Table 13.

Table 13: Examples of questions and answers from four visual perception tasks.

Visual Perception Task	Question	Answer
Object Classification	<i>what are sitting down on the ground</i>	<i>bears</i>
	<i>what is parked on the side of the grass</i>	<i>motorcycle</i>
	<i>what are two https://www.overleaf.com/project/64eb0aa69f2b1a658d35a15ben playing with some elephants</i>	<i>ball</i>
	<i>what is the color of the shirt</i>	<i>blue</i>
Counting	<i>what is laying on the bed next to some pillows</i>	<i>cat</i>
	<i>how many men is sitting on the street in front of a building</i>	<i>two</i>
	<i>how many red velvet cup cakes with no frosting on a flowered plate</i>	<i>three</i>
	<i>how many pairs of shoes on a mat with a cat is sitting in the middle</i>	<i>eight</i>
	<i>how many dessert treats in the white cardboard box</i>	<i>six</i>
Color Recognition	<i>how many trays of itallian food are in large pans</i>	<i>four</i>
	<i>what is the color of the airplane</i>	<i>black</i>
	<i>what is the color of the motorcycle</i>	<i>orange</i>
	<i>what is the color of the brush</i>	<i>green</i>
Position Reasoning	<i>what is the color of the bird</i>	<i>white</i>
	<i>what is the color of the flowers</i>	<i>red</i>
	<i>where is the cat lounging</i>	<i>chair</i>
	<i>where do the mother and son make sundaes</i>	<i>kitchen</i>
	<i>where is the cheese pizza</i>	<i>box</i>
Position Reasoning	<i>where is the person sitting</i>	<i>bed</i>
	<i>where do the large and over-sized stuffed teddy bear sitting</i>	<i>chair</i>

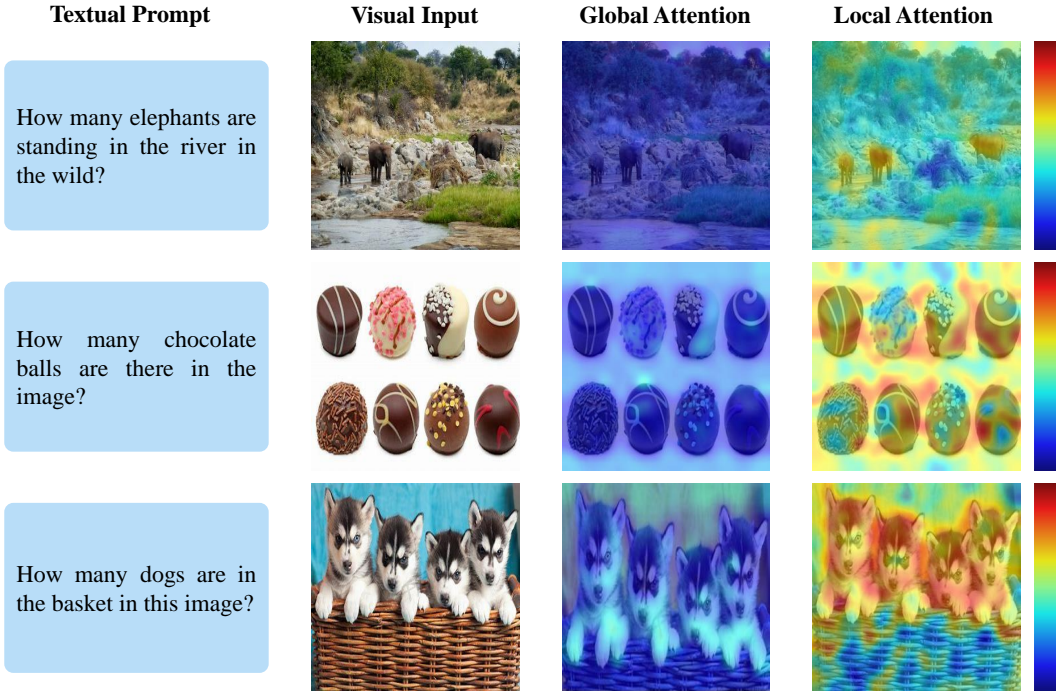


Figure 8: Visualization of prompt-aware global and local attention on counting task. Visualization results show that global attention spans the entire prompt content, while local attention concentrates predominantly on the specific object in question. Our method performs well in accurately identifying and counting objects.

E.2 MME Benchmark

MME [23] benchmark evaluates both the perception and cognition abilities of MLLMs. In addition to OCR, perception encompasses the recognition of both coarse-grained and fine-grained objects. Coarse-grained recognition includes the identification of objects’ existence, count, position, and color. Fine-grained recognition involves identifying movie posters, celebrities, scenes, landmarks, and artworks. Cognition tasks include commonsense reasoning, numerical calculation, text translation, and code reasoning. There are a total of 14 sub-tasks, detailed as follows.

Coarse-Grained Recognition. The contents of coarse-grained recognition include identifying the existence of common objects and determining their count, color, and position. Images are sourced from the COCO dataset [63], but all instruction-answer pairs are manually constructed rather than directly using available annotations. Even if MLLMs have previously encountered these COCO images, the manually prepared pairs are not included in their training sets. This setup requires MLLMs to comprehend the instructions and infer the correct answers. For each perception subtask of existence, count, color, and position, 30 images are used, with a total of 60 instruction-answer pairs prepared.

Fine-Grained Recognition. Fine-grained recognition evaluates the knowledge resources of MLLMs, encompassing subtasks such as recognizing movie posters, celebrities, scenes, landmarks, and artworks. These subtasks include 147, 170, 200, 200, and 200 images respectively. For the celebrity subtask, a red box is placed around a person with a clearly visible face in the image, with the instruction being, “Is the actor inside the red box named [celebrity name]? Please answer yes or no.” Similar to the coarse-grained recognition, images for these subtasks are sourced from publicly available datasets [78, 79, 80, 81, 82], and all instructions are manually crafted.

Optical Character Recognition. Optical Character Recognition (OCR) is a foundational capability of MLLMs, supporting subsequent text-based tasks such as text translation and text understanding. Images are sampled from [83], with all instruction-answer pairs manually designed. Given that MLLMs are still in their early stages, only relatively simple samples are chosen for this version of MME. This section includes 20 images and 40 instruction-answer pairs.

All image-prompt-answer pairs are manually created. The few public datasets used in this benchmark utilize only the images without relying on their original annotations. Additionally, images are collected through real photographs and image generation. The prompts in MME are designed to be concise to minimize the influence of

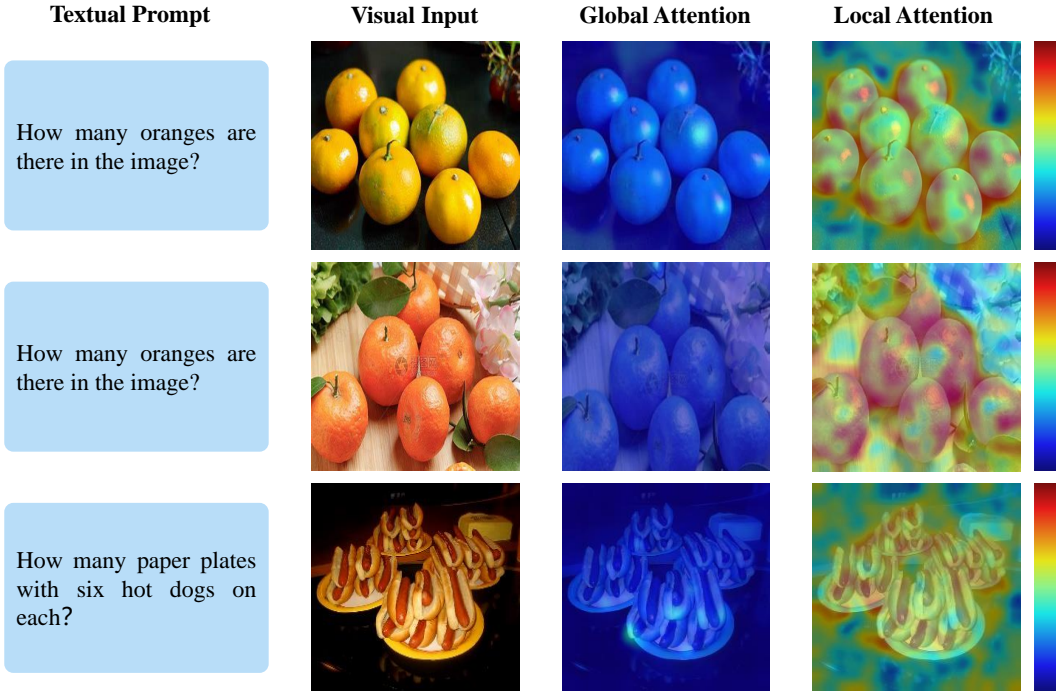


Figure 9: Visualization of prompt-aware global and local attention on counting task. Visualization results show that global attention spans the entire prompt content, while local attention concentrates predominantly on the specific object in question. Our method performs well in accurately identifying and counting objects.

prompt engineering on the model’s output. Due to the instruction design of “please answer yes or no” quantitative statistics can be easily performed based on the “yes” or “no” responses from MLLMs, ensuring accuracy and objectivity.

F Prompts used for Fine-tuning

The prompt templates employed in the end-to-end prompt fine-tuning process across various tasks are illustrated in Table 14.

Table 14: Prompt templates used for converting datasets into prompt-tuning data. In VQA tasks, two formats of prompts are available. Note that the “{Question}” format is mandatory for the prompt-aware adapter, and needs to be replaced with the specific question in Table 13.

Task	Prompt Template
Image Captioning	<code>[INST] <Image Feature> [Caption] <Describe this image in detail.> [/INST]</code>
	<code>[INST] <Image Feature> [Caption] <Take a look at this image and describe what you notice.> [/INST]</code>
	<code>[INST] <Image Feature> [Caption] <Please provide a detailed description of the picture.> [/INST]</code>
	<code>[INST] <Image Feature> [Caption] <Could you describe the contents of this image for me?> [/INST]</code>
	<code>[INST] <Image Feature> [Caption] <Is this image common in real world?> [/INST]</code>
Visual Question Answering	<code>[INST] <Image Feature> [vqa] <Describe this image in detail. > [/INST]</code>
	<code>[INST] <Image Feature> [vqa] <Take a look at this image and describe what you notice. > [/INST]</code>
	<code>[INST] <Image Feature> [vqa] <Could you describe the contents of this image for me? > [/INST]</code>
	<code>[INST] <Image Feature> [vqa] <Is this image common in real world? > [/INST]</code>
	<code>[INST] <Image Feature> [vqa] <Question > [/INST]</code>

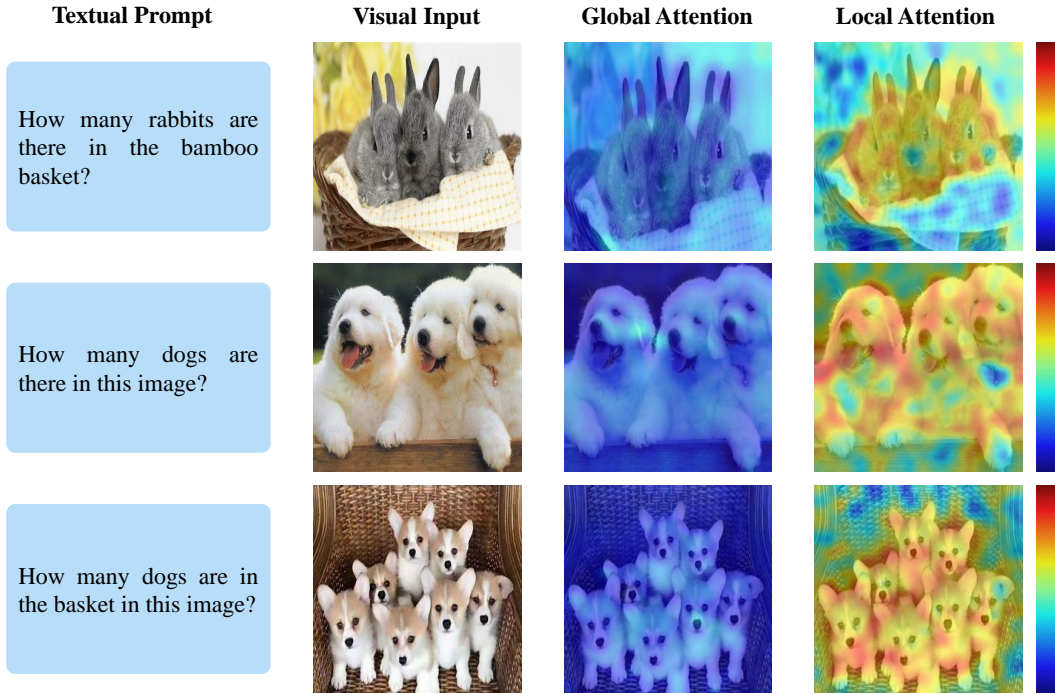


Figure 10: Visualization of prompt-aware global and local attention on counting task. Visualization results show that global attention spans the entire prompt content, while local attention concentrates predominantly on the specific object in question. Our method performs well in accurately identifying and counting objects.

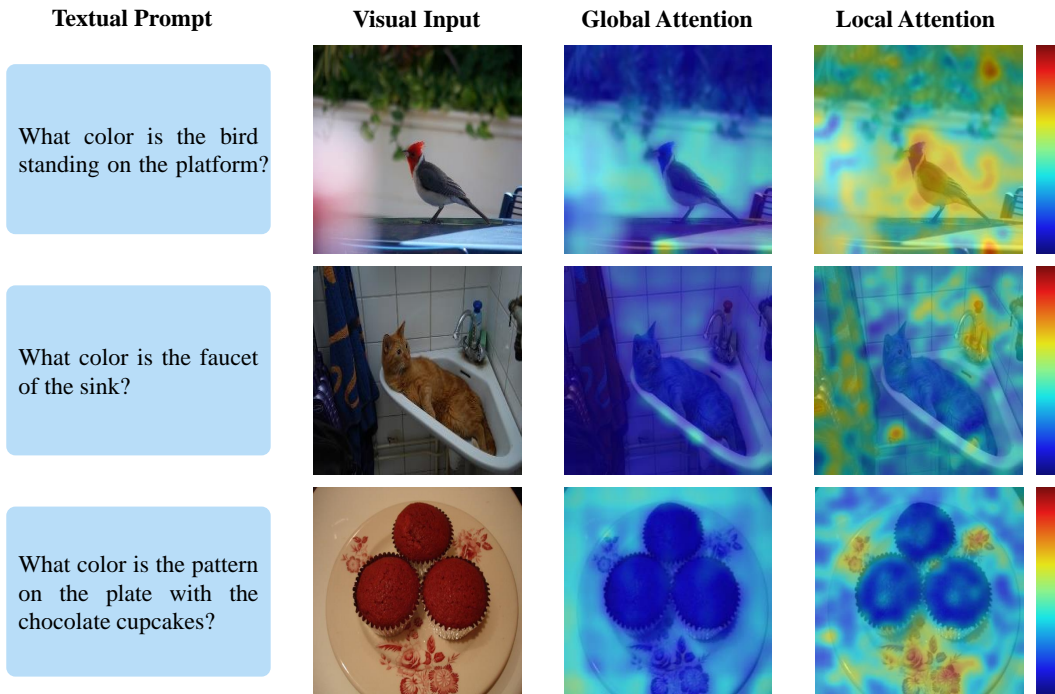


Figure 11: Visualization of prompt-aware global and local attention on the color recognition task. Visualization results show that global attention spans the entire prompt content, while local attention concentrates predominantly on the specific object in question. Our method achieves impressive performance in accurately identifying and distinguishing colors.

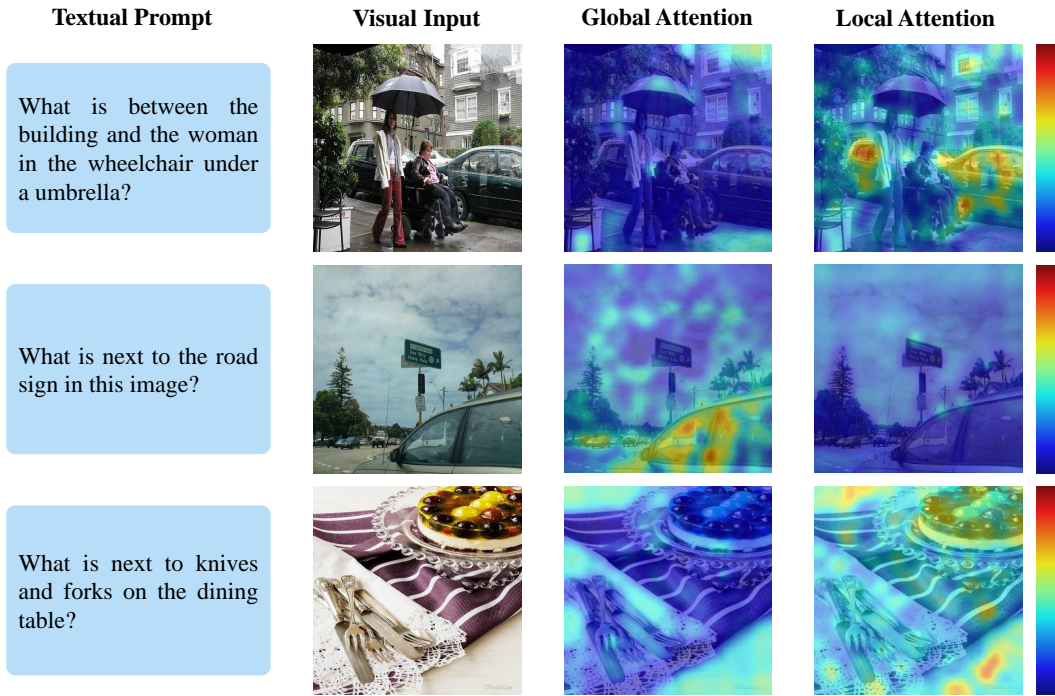


Figure 12: Visualization of prompt-aware global and local attention on the position reasoning task. Visualization results show that global attention spans the entire prompt content, while local attention concentrates predominantly on the specific object in question. Our method has the capability of location recognition.

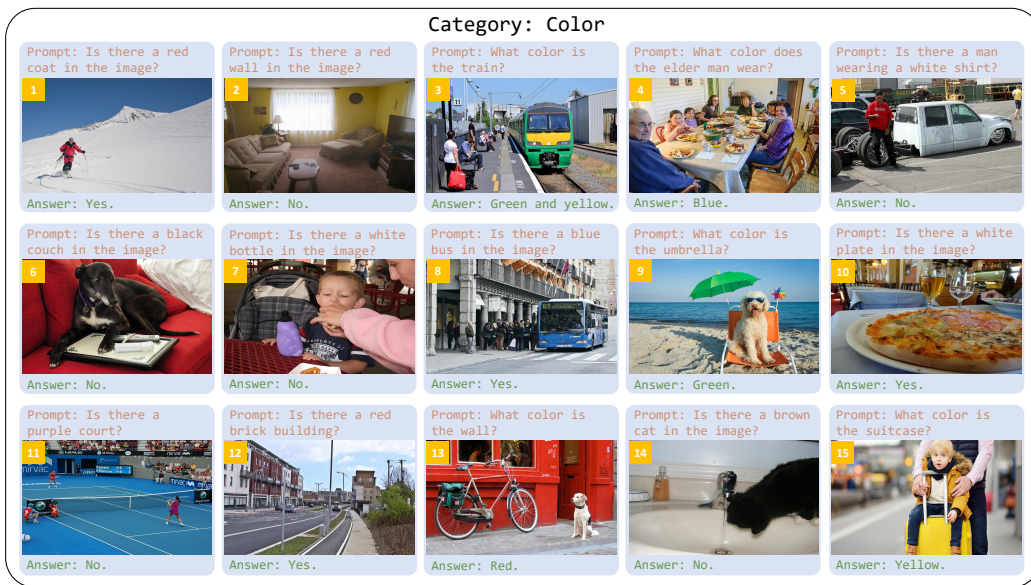


Figure 13: Zero-shot image-to-text generation using an MLLM based on the prompt-aware adapter, where it shows favorable visual perception ability on the color recognition task.



Figure 14: Zero-shot image-to-text generation using an MLLM based on the prompt-aware adapter, where it shows favorable visual perception ability on the counting task.

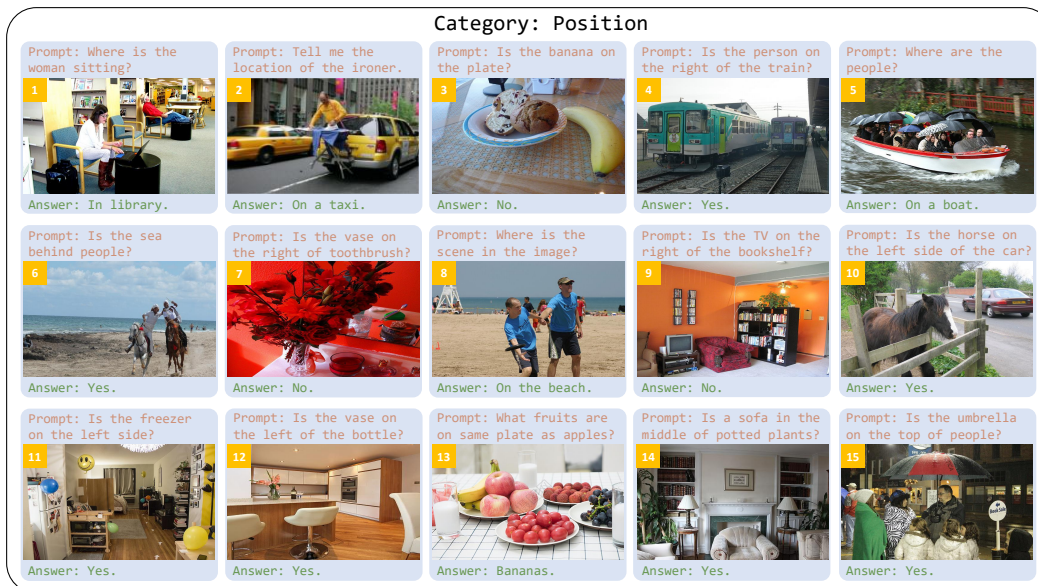


Figure 15: Zero-shot image-to-text generation using an MLLM based on the prompt-aware adapter, where it shows favorable visual perception ability on the position reasoning task.

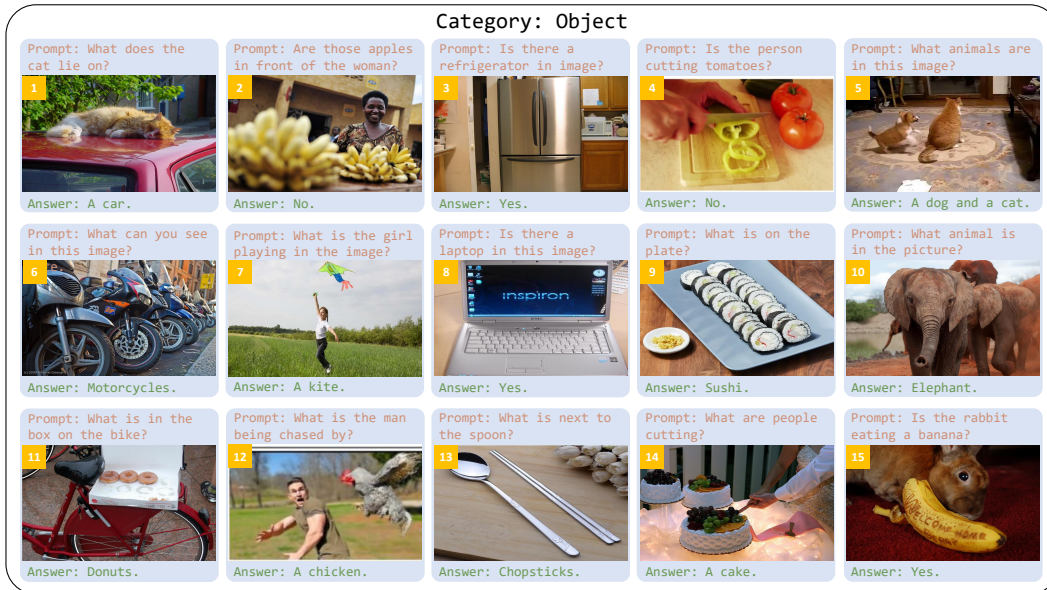


Figure 16: Zero-shot image-to-text generation using an MLLM based on the prompt-aware adapter, where it shows favorable visual perception ability on the object detection task.

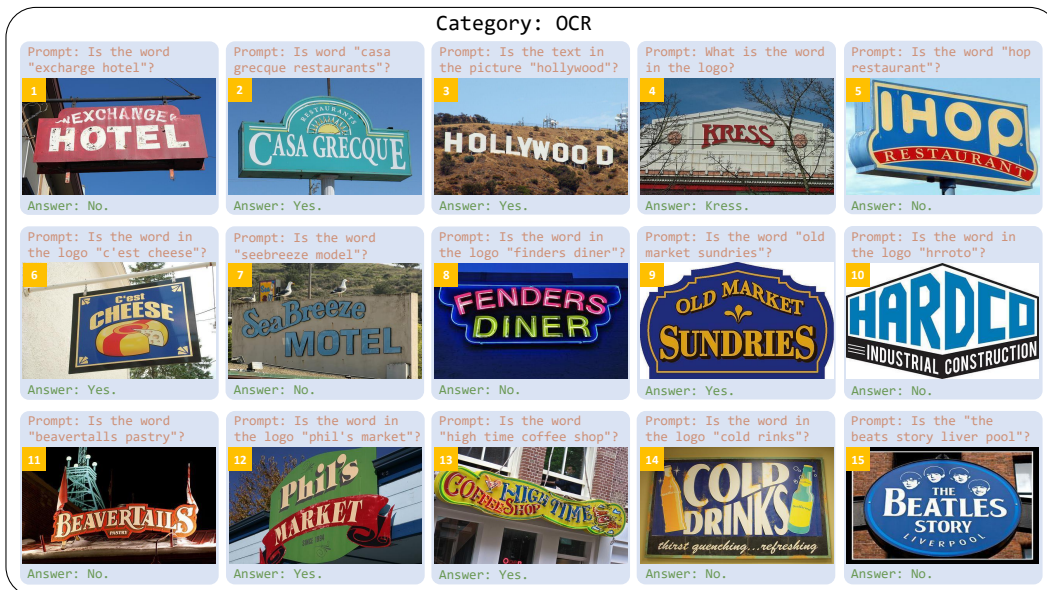


Figure 17: Zero-shot image-to-text generation using an MLLM based on the prompt-aware adapter, where it shows favorable visual perception ability on the OCR task.

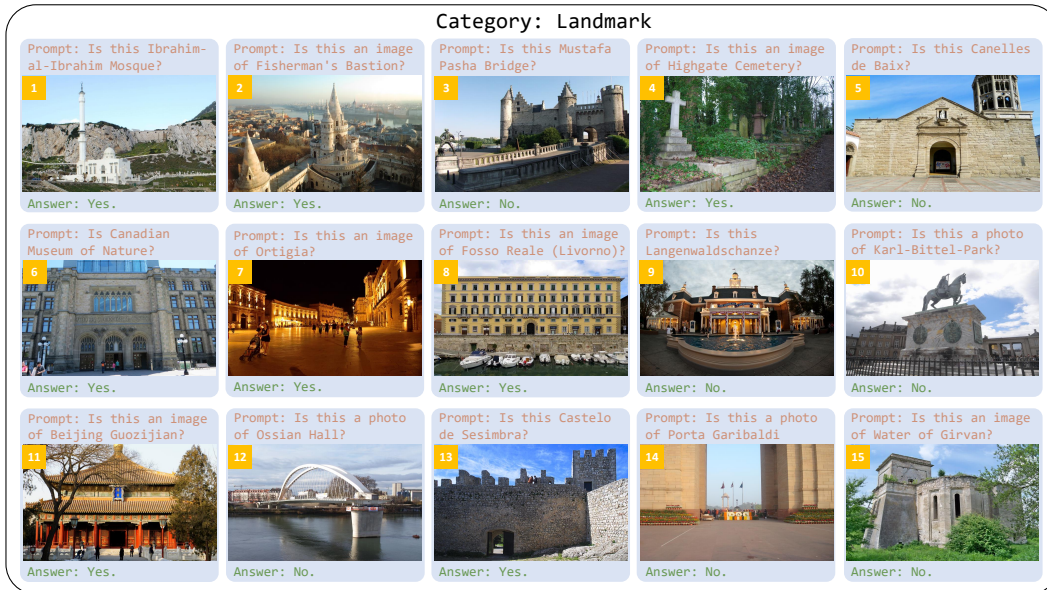


Figure 18: Zero-shot image-to-text generation using an MLLM based on the prompt-aware adapter, where it shows favorable visual perception ability on the landmark recognition task.



Figure 19: Zero-shot image-to-text generation using an MLLM based on the prompt-aware adapter, where it shows favorable visual perception ability on the celebrity recognition task.

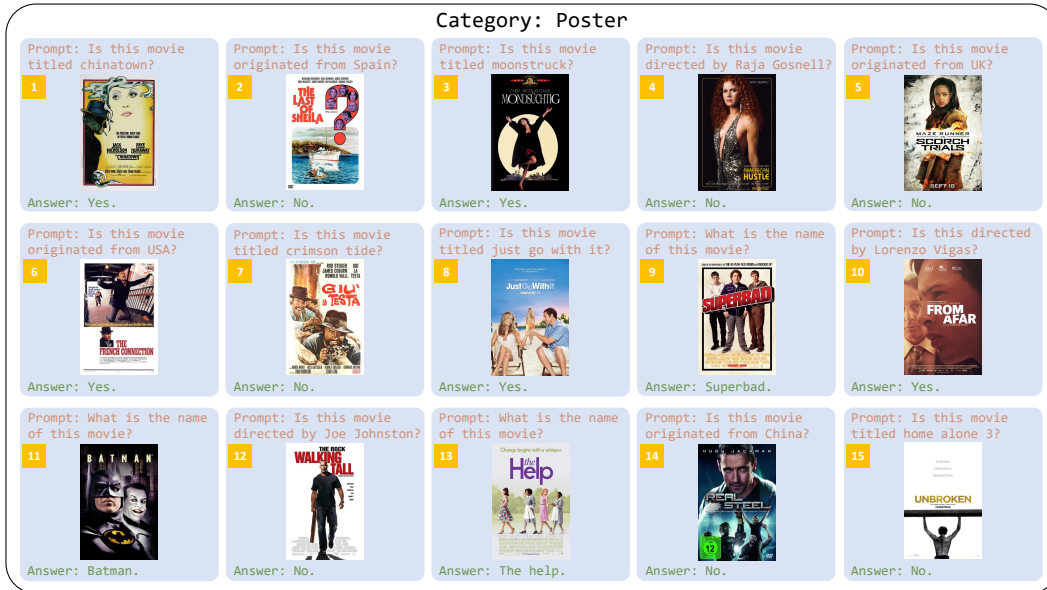


Figure 20: Zero-shot image-to-text generation using an MLLM based on the poster recognition task.

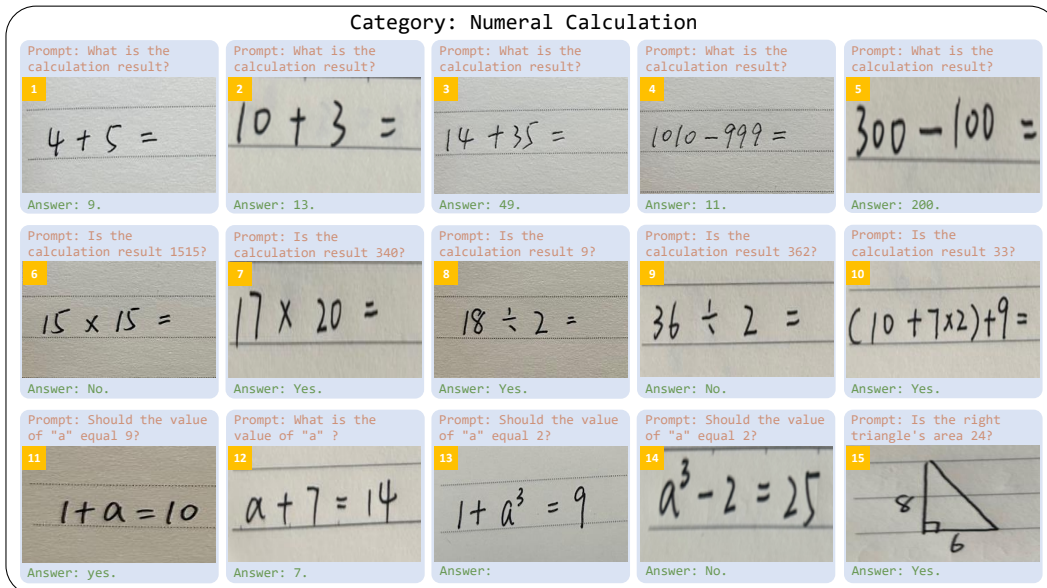


Figure 21: Zero-shot image-to-text generation using an MLLM based on the prompt-aware adapter, where it shows favorable visual cognition ability on the calculation task.

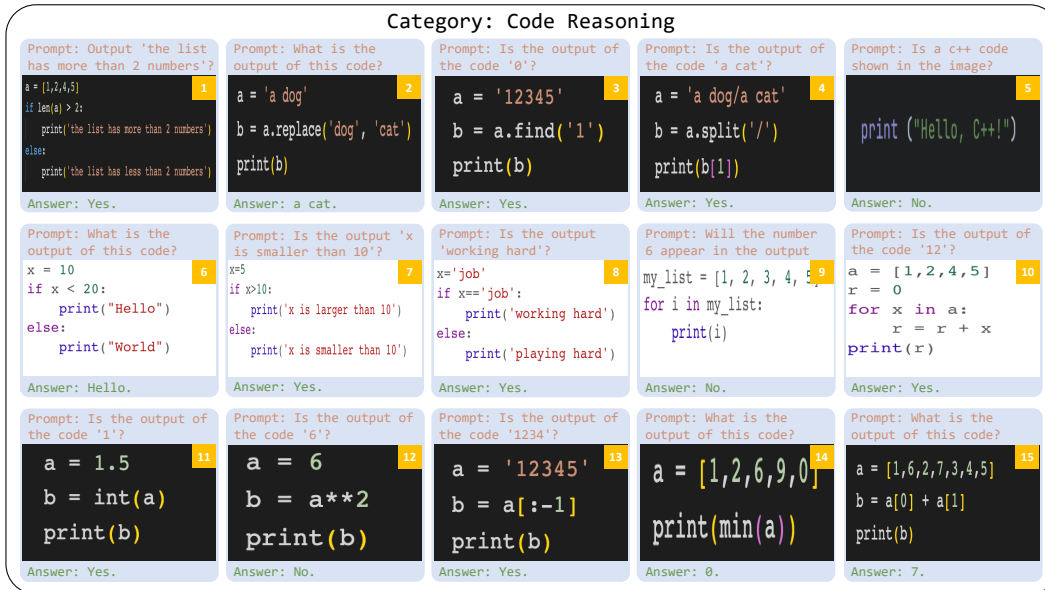


Figure 22: Zero-shot image-to-text generation using an MLLM based on the prompt-aware adapter, where it shows favorable visual cognition ability on the code reasoning task.



Figure 23: Zero-shot image-to-text generation using an MLLM based on the prompt-aware adapter, where it shows favorable visual cognition ability on the commonsense reasoning task.

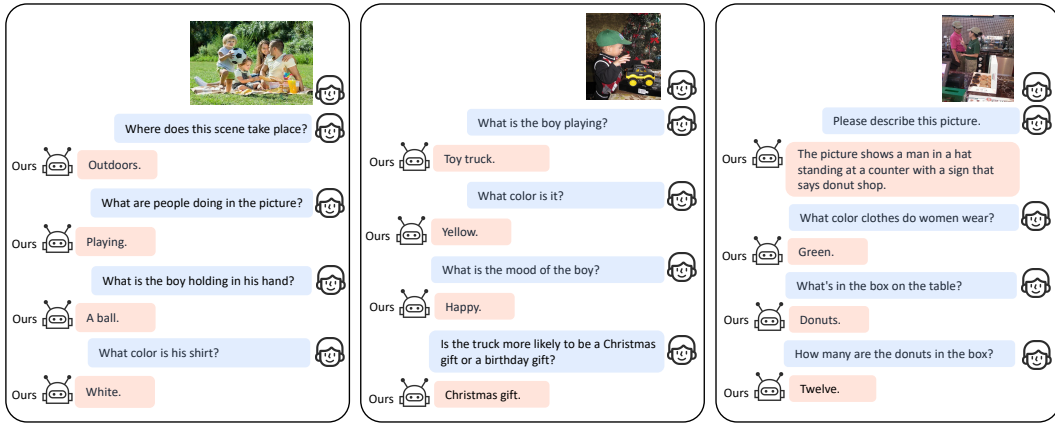


Figure 24: Zero-shot image-to-text generation using an MLLM based on the prompt-aware adapter, where it shows favorable visual perception ability.

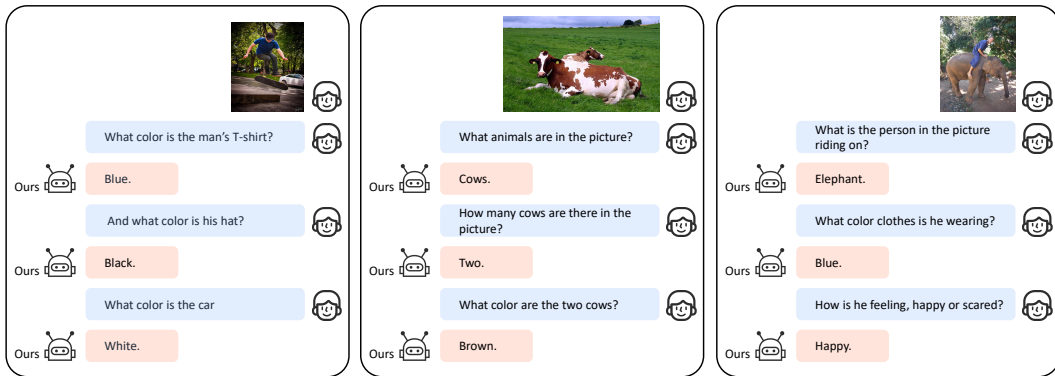


Figure 25: Zero-shot image-to-text generation using an MLLM based on the prompt-aware adapter, where it shows favorable visual perception ability.

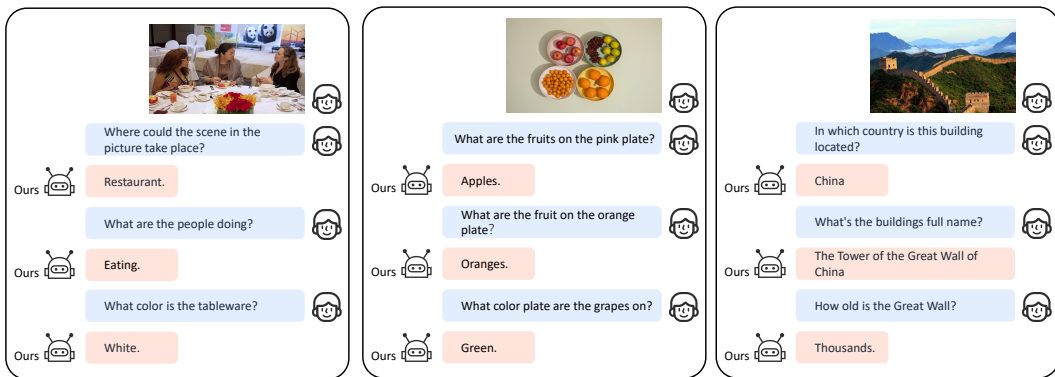


Figure 26: Zero-shot image-to-text generation using an MLLM based on the prompt-aware adapter, where it shows favorable visual perception ability.